

1-1-1994

## A study of recognition coating response for quartz crystal microbalances

Robert Louis Curiale  
*University of Nevada, Las Vegas*

Follow this and additional works at: <https://digitalscholarship.unlv.edu/rtds>

---

### Repository Citation

Curiale, Robert Louis, "A study of recognition coating response for quartz crystal microbalances" (1994). *UNLV Retrospective Theses & Dissertations*. 439.  
<http://dx.doi.org/10.25669/se21-2z2e>

This Thesis is protected by copyright and/or related rights. It has been brought to you by Digital Scholarship@UNLV with permission from the rights-holder(s). You are free to use this Thesis in any way that is permitted by the copyright and related rights legislation that applies to your use. For other uses you need to obtain permission from the rights-holder(s) directly, unless additional rights are indicated by a Creative Commons license in the record and/or on the work itself.

This Thesis has been accepted for inclusion in UNLV Retrospective Theses & Dissertations by an authorized administrator of Digital Scholarship@UNLV. For more information, please contact [digitalscholarship@unlv.edu](mailto:digitalscholarship@unlv.edu).

## **INFORMATION TO USERS**

**This manuscript has been reproduced from the microfilm master. UMI films the text directly from the original or copy submitted. Thus, some thesis and dissertation copies are in typewriter face, while others may be from any type of computer printer.**

**The quality of this reproduction is dependent upon the quality of the copy submitted. Broken or indistinct print, colored or poor quality illustrations and photographs, print bleedthrough, substandard margins, and improper alignment can adversely affect reproduction.**

**In the unlikely event that the author did not send UMI a complete manuscript and there are missing pages, these will be noted. Also, if unauthorized copyright material had to be removed, a note will indicate the deletion.**

**Oversize materials (e.g., maps, drawings, charts) are reproduced by sectioning the original, beginning at the upper left-hand corner and continuing from left to right in equal sections with small overlaps. Each original is also photographed in one exposure and is included in reduced form at the back of the book.**

**Photographs included in the original manuscript have been reproduced xerographically in this copy. Higher quality 6" x 9" black and white photographic prints are available for any photographs or illustrations appearing in this copy for an additional charge. Contact UMI directly to order.**

# **UMI**

A Bell & Howell Information Company  
300 North Zeeb Road, Ann Arbor, MI 48106-1346 USA  
313/761-4700 800/521-0600



**A STUDY OF RECOGNITION COATING  
RESPONSE FOR QUARTZ CRYSTAL  
MICROBALANCES**

by

**Robert Louis Curiale**

**A thesis submitted in partial fulfillment  
of the requirements for the degree of**

**Master of Science**

**in**

**Chemistry**

**Department of Chemistry  
University of Nevada, Las Vegas  
December 1994**

UMI Number: 1374868

Copyright 1994 by  
Curiale, Robert Louis  
All rights reserved.

---

UMI Microform 1374868  
Copyright 1995, by UMI Company. All rights reserved.

This microform edition is protected against unauthorized  
copying under Title 17, United States Code.

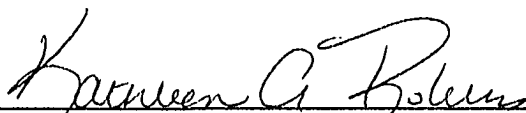
---


UMI

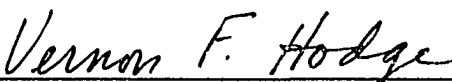
300 North Zeeb Road  
Ann Arbor, MI 48103

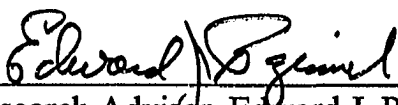
**©1994 Robert L. Curiale  
All Rights Reserved**


The Thesis of Robert L. Curiale for the degree of Master of Science in Chemistry is approved.


  
Chairperson, Kathleen A. Robins, Ph.D.

  
Examining Committee Member, David W. Emerson, Ph.D.

  
Examining Committee Member, Vernon F. Hodge, Ph.D.

  
Research Advisor, Edward J. Poziomek, Ph.D.

  
Graduate Faculty Representative, Donald H. Baepler, Ph.D.

  
Dean of the Graduate College, Cheryl L. Bowles, Ed.D.

University of Nevada, Las Vegas  
December 1994

## ABSTRACT

Computerized molecular modeling methods supplemented with chemometric methods may be used to provide information regarding sensitivity, selectivity, and other properties of solid/vapor sorption interactions for chemically coated Quartz Crystal Microbalances (QCMs). When exposed to the individual vapors of a homologous series of carboxylic acid vapors, a QCM coated with varying thicknesses of poly(ethylenimine) (PEI) coating, produces a linear response that is sensitive and selective. The selectivity of the PEI coating toward analytes increases with aliphatic chain length probably due to dispersive interactions. A linear relationship between calculated van der Waals force values and experimental dispersion force values may exist. BET isotherm plots indicate that heats of adsorption values for the interactions fall within the range of physical adsorption. At high analyte concentrations, PEI coated sensors may behave differently because multilayering interactions increase. At low concentrations, monolayer adsorption appears to predominate and the values of the coating coefficients become constant.



## TABLE OF CONTENTS

ABSTRACT.....	iii
LIST OF FIGURES.....	vi
FOREWORD.....	viii
Notice .....	ix
Acknowledgements .....	ix
Chapter 1 - INTRODUCTION .....	1
General .....	1
A Law Enforcement Scenario Related to Drug Interdiction.....	2
Quartz Crystal Microbalance.....	6
Definition .....	6
Piezoelectric Effect .....	6
Piezoelectric Quartz Crystal Resonators .....	7
Mass Determination by a Quartz Crystal Microbalance .....	11
General Formulas for Mass Determination by a Quartz Crystal Microbalance .....	11
Design Considerations.....	13
Solid/Vapor Interactions.....	13
Gas-Liquid Chromatography .....	15
Partition Coefficient .....	15
Factors that Influence Retention .....	16
Choice of Stationary Phase.....	17
Linear Solvation Energy Relationships .....	19
Polarizability .....	20
Dipolarity .....	21
Hydrogen Bonding .....	21
London's Dispersion Forces.....	22
Cavity Effects.....	22

Sorption Isotherms .....	23
General .....	23
Monolayer Adsorption - The Langmuir Isotherm .....	24
Multilayer Adsorption - The Brunauer-Emmet-Teller Isotherm .....	24
Chapter 2 - OBJECTIVES AND HYPOTHESIS.....	27
Objectives .....	27
Hypothesis .....	27
Chapter 3 - EXPERIMENTAL.....	29
Methods and Materials .....	29
Materials and Equipment.....	29
Vapor Generator Calibration .....	30
Recognition Coating Study .....	31
Film Thickness and Sensitivity .....	31
Analyte Studies .....	33
Isotherm Determination .....	33
Dilution Effects and Coating Sensitivity .....	34
Chapter 4 - RESULTS AND DISCUSSION .....	35
Recognition Coating Study .....	35
Film Thickness and Sensitivity .....	35
Analyte Studies .....	40
Isotherm Determination .....	40
Dilution Effects and Coating Sensitivity .....	48
Molecular Orientation .....	50
Chapter 5 - SUMMARY AND CONCLUSIONS.....	52
Chapter 6 - FUTURE WORK .....	55
APPENDIX I .....	57
Raw Data and Calculations .....	57
APPENDIX II.....	72
Additional Data Tables and Figures.....	72
APPENDIX III.....	81
Molecular Modeling Software Information .....	81
BIBLIOGRAPHY .....	85

## LIST OF FIGURES

Figure 1. Molecular structure of cocaine hydrochloride and cocaine .....	3
Figure 2. A quartz crystal in its perfect natural form. ....	8
Figure 3. The fundamental thickness-shear mode of vibration .....	9
Figure 4. AT- cut, BT- cut, and SC- cut quartz crystal plates .....	10
Figure 5. Typical cemented lead type 10 MHz AT- cut silicon coated quartz crystal microbalance with gold electrodes. ....	14
Figure 6. Corrosive vapor generator designed and built by Dominguez, Lin, and Li. ....	30
Figure 7. A typical 10 MHz QCM frequency response curve showing the baseline and introduction of alternating 40 second pulses of benzoic acid vapors and nitrogen purge. ....	32
Figure 8. Poly(ethylenimine) coating thickness versus frequency response for a homologous series of carboxylic acids using a 10MHz QCM. ....	37
Figure 9. Relationship of experimentally obtained dispersion force slope values versus calculated Van der Waals force values for an homologous series of carboxylic acids .....	38
Figure 10. Typical isotherm of poly(ethylenimine) coated 10 MHz QCM frequency response to acetic acid vapors. ....	40
Figure 11. Isotherm plot for formic acid interaction with 2.0 KHz PEI coated 10 MHz QCM. ....	41

Figure 12. Isotherm plot for acetic acid interaction with 2.0 KHz PEI coated 10 MHz QCM.....	42
Figure 13. Isotherm plot for propanoic acid interaction with 2.0 KHz PEI coated 10 MHz QCM.....	42
Figure 14. Isotherm plot for butanoic acid interaction with 2.0 KHz PEI coated 10 MHz QCM.....	43
Figure 15. Combined isotherm plot for formic, acetic, propanoic, and butanoic acids interactions with 2.0 KHz PEI coated 10 MHz QCM.....	43
Figure 16. Linearized form of BET isotherm for formic acid interaction with 2.0 KHz PEI coated 10 MHz QCM.....	45
Figure 17. Linearized form of BET isotherm for acetic acid interaction with 2.0 KHz PEI coated 10 MHz QCM.....	45
Figure 18. Linearized form of BET isotherm for propanoic acid interaction with 2.0 KHz PEI coated 10 MHz QCM.....	46
Figure 19. Linearized form of BET isotherm for butanoic acid interaction with 2.0 KHz PEI coated 10 MHz QCM.....	46
Figure 20. Combined linearized forms of BET isotherms for formic, acetic, propanoic, and butanoic acids interactions with 2.0 KHz PEI coated 10 MHz QCM.....	47
Figure 21. The effects of methylene addition to calculated changes in heats of adsorptions for formic, acetic, propanoic, and butanoic acids interactions with 2.0 KHz PEI coated 10 MHz QCM.....	47
Figure 22. Plot indicating the variance of PEI coating coefficient values at six dilutions for formic, acetic, propanoic, butanoic, pentanoic, and hexanoic acids, a homologous series. ....	49

## **FOREWORD**

The research for this thesis is sponsored by the Department of Defense (DoD) Advanced Research Project Agency (ARPA) Experimental Program to Stimulate Competitive Research (EPSCoR) (Contract No. DAAD05-92-C0286). It is designed to complement ARPA parent contract DAAD05-92-C-0027. The objective of the parent contract is to assist in the technology development and design of a chemical vapor detector system based on emerging chemical microsensor and microinstrument technology, specifically chemical mass sensors.

The DARPA EPSCoR research plan is designed to complement the parent contractual effort through the following tasks:

- Perform molecular modeling studies involving candidate recognition coatings and various organic analytes of drug interdiction interest to obtain best fit for molecular association to optimize selectivity and sensitivity.
- Evaluate promising candidate recognition coatings with a chemical mass sensor system.

The UNLV Project Officer is Dr. Edward J. Poziomek, Harry Reid Center for Environmental Studies. The DoD's Project Officer is James Petrousky, Naval Explosive Ordnance Disposal Technology Center, Indian Head, MD. The Faculty Advisor is Dr. Kathleen A. Robins, Department of Chemistry, UNLV.

### **Notice**

Although the information in this paper has been funded by the U.S. Department of Defense under Contract No. DAAD05-92-C0286 with the University of Nevada -Las Vegas, it does not necessarily reflect the view of the DoD, and no official endorsement should be inferred.

### **Acknowledgements**

I personally wish to thank the numerous persons and organizations which have contributed to this thesis.

- Martha E. Dominguez (colleague and co-investigator)
- Dr. Edward J. Poziomek (research advisor)
- Dr. Kathleen A. Robins, (committee chair and advisor)
- Dr. David W. Emerson, Dr. Vernon F. Hodge, and Dr. Donald H. Baeppler (committee members)
- Dr. Spencer M. Steinberg (technical consultant and advisor)
- Shirley Burns (graphic artist)
- Dennis L. Stevens (colleague)
- Edward C. Baxter (computer assistance)
- Harry Reid Center for Environmental Studies at the University of Nevada, Las Vegas (UNLV) for the use of their facilities.
- Advanced Research Projects Agency (ARPA) Experimental Program to Stimulate Competitive Research (EPSCOR) for funding the research.

## Chapter 1

### INTRODUCTION

#### General

Quartz Crystal Microbalance (QCM) sensor technology that incorporates the use of sensitive and selective chemical sensor recognition coatings can provide a means for rapid identification and quantification of specific analyte vapors. The chemical recognition coatings are deposited on the surfaces of the mass-sensitive QCM devices. Some analyte vapors may interact more strongly with the coatings than others. Sorption onto/into the coatings and or chemical reaction with the coatings increases the surface mass on the QCM. The change in mass results in surface deformation of the resonating quartz crystal which can be detected and monitored using a frequency counting apparatus.

Selection of recognition coatings that react specifically with low concentrations of the target analytes is a major technology challenge. Understanding the molecular interactions which occur between coatings and analytes should provide a basis for recognition coating selection. Various tradeoffs involving sensitivity, specificity, reversibility, ease of coating deposition, coating thickness, etc. must be considered when designing, chemical mass sensor systems.

Molecular mechanics and computer modeling have become powerful tools for attempting to understand the structures, properties, mechanisms, and kinetics of molecular interactions. This thesis research addresses the challenge of selecting recognition coatings for chemical mass sensor systems.

The basis for funding this research came from a need to develop a low cost, rapid, non-intrusive sensor for cocaine and cocaine hydrochloride. A mass sensor system was selected and research on recognition coatings including the present thesis work was initiated. If molecular modeling proves useful in predicting sensitivity, selectivity and other related aspects of recognition coating/analyte interactions, there are many technology transfer possibilities. There is a need for low cost, rapid, screening and monitoring mass sensors in many areas including hazardous material site cleanup, remediation, law enforcement for detection of explosives, industrial process monitoring, and workplace monitoring to name a few. The following section illustrates the process of selecting a potential coating for a sensor application. The research in this thesis addresses needs for sensor recognition coatings involving a drug interdiction law-enforcement scenario which is described in more detail below.

### **A Law-Enforcement Scenario Related to Drug Interdiction**

Cocaine and cocaine hydrochloride have become primary drugs of abuse. Interdiction of illicitly processed cocaine is a primary objective of several Federal agencies. Non-intrusive methods for detection of cocaine



hidden in containers, import cargoes or detection in the areas of clandestine laboratories are needed. The increased sophistication of cocaine smuggling and trafficking techniques warrants research and development of new technologies and strategies for drug enforcement agencies.<sup>1</sup>

Production, packaging and storage of illicit cocaine varies immensely; numerous impurities and artifacts may be detected through forensic analyses.<sup>2,3</sup> Illicit cocaine is primarily smuggled in the form of the hydrochloride salt. In pure form it is water soluble (1.0 g cocaine-HCl/0.4mL H<sub>2</sub>O)<sup>4</sup> and exhibits a low vapor pressure. (ca.  $2 \times 10^{-7}$  Torr)<sup>5</sup> At ambient temperatures, trained dogs may detect cocaine; humans cannot.<sup>6</sup>

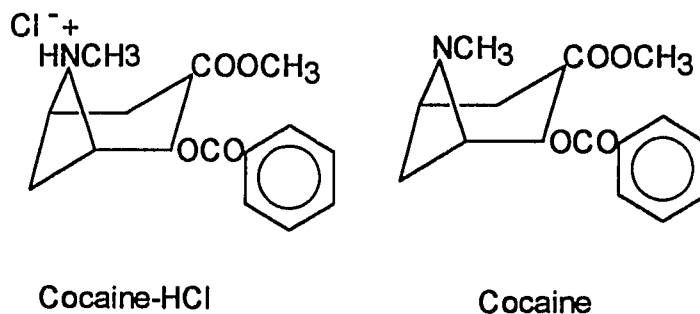


**Figure 1.** Molecular structure of cocaine hydrochloride and cocaine.

A new strategy for the detection and identification of cocaine hydrochloride was conceived by E. J. Poziomek and H. Wohltjen under ARPA Contract No. DAAD05-92-C-0027. It involves the collection/sampling of cocaine hydrochloride followed by pyrolysis into vapors that can be detected by mass sensors. The major pyrolytic decomposition products of *l*-cocaine at 600 °C under a N<sub>2</sub> atmosphere have been identified in an attempt to assess the compounds that a cocaine smoker

might be exposed to. These include benzoic acid, ethene, and methylamine. Numerous decomposition products have also been identified. (See Table 1.)<sup>7</sup> Benzoic acid was the major component. Cocaine-HCl decomposition products at ~150-350 °C under a N<sub>2</sub> atmosphere are benzoic acid, methylamine, carboxymethylcycloheptatriene, hydrochloric acid.<sup>8</sup> Pyrolysis of cocaine-HCl at ~200-300°C under an air atmosphere have yielded decomposition products identified as benzoic acid, methylamine, methyl cycloheptatriencarboxylate, carbonyl compounds (aldehydes and ketones) and hydrochloric acid.

**Table 1.**

Components identified by Novak *et al* in the pyrolysate of cocaine<sup>a</sup> under a nitrogen atmosphere at 600°C

Compound	%
Phenol	0.2
Methyl benzoate	0.06
Methyl nicotinate	0.1
Methyl phenylacetate	0.7
Methyl <i>o</i> -toluate	0.04
Benzoic acid	52.0
Methyl <i>m</i> -toluate	0.07
Methyl <i>p</i> -toluate	0.2
Methyl 2-methyl nicotinate	trace
A methyl cycloheptatrienecarboxylate	trace
Methyl 6-methylnicotinate	0.05
(2- <i>exo</i> )-8-Methyl-8-azabicyclo[3.2.1]	0.2
oct-3-ene-2-carboxylic acid methyl ester	
Methyl 2-(3-pyridyl)butanoate	trace
Methylecgonidine	0.3
Methyl 4-(3-pyridyl)butanoate	7.0
Cocaine	37.6

<sup>a</sup> The naturally occurring form *l*-cocaine was investigated.

The studies in this thesis focus on the aspects of the sensitivity, selectivity, and reversibility of several organic analytes of interest interactions with one particular chemical recognition coating. Formic, acetic, propanoic, butanoic, pentanoic, and hexanoic acids, a homologous series of carboxylic acids, were selected to mimic and differentiate the response associated with benzoic acid, a major byproduct in cocaine pyrolysis. Except for benzoic acid, all of the acids are liquids at room temperature which facilitated vapor generation to the mass sensor. Several types of recognition coatings such as poly-4-vinylpyridine, ethylenediamine, and poly(ethylenimine) (PEI) to name a few were previously evaluated on the QCM. The latter, PEI, not only exhibited one of the the highest interaction sensitivities with acid analytes but also showed good stability over time, a major sensor coating design consideration. Therefore, PEI coating was used in the studies.

It is interesting to note that molecular mechanics methods have already been used to study the molecular interaction of cocaine with a glycine substrate.<sup>9</sup> Such properties as bond lengths, bond angles, and atomic charges for both structures have been calculated and are in accordance with *ab initio* values.<sup>10</sup> Geometry optimizations predict that the piperidine ring of cocaine adopts a chair conformation with the *N*-methyl group being equatorial. This coincides with experimental X-ray powder defraction results obtained by Hrynychuk.<sup>11</sup> Nucleophilic attack sequences based on charge interactions were investigated and found to be in accord with present day theory.<sup>12</sup> Heats of formation of various species were calculated; however, no experimental equivalent has been located for comparison.

## Quartz Crystal Microbalance

### Definition

A quartz crystal microbalance (QCM) is a piezoelectric material which is used to measure mass. QCMs have been used for numerous applications; some of these applications include monitoring thin film deposition in process control, simultaneous measurement of mass and temperature, determination of chemisorption and physical adsorption in surface science, monitoring of plasma-assisted etching determinations, gas chromatograph detectors, sorption detectors, space system contamination studies, and in aerosol mass measurement. Other investigators have used QCM's for interferometric studies, humidity sensing, dew points of gases, a manometer, corrosion studies of metal films, polymerization of butadiene, measuring contaminants in vacuum systems, oxidation of elastomers, and detecting phosphonates by mercury bromide coated crystals. One of the first sensor applications was by King in 1964 who developed a vapor detector for the Mariner space probe to detect water vapors in the Martian atmosphere.<sup>13</sup> The present thesis research utilizes QCMs for measuring organic vapor sorption as part of chemical sensor applications.

### Piezoelectric Effect

Pierre and Jacques Curie discovered the concept of piezoelectricity ("pressure"+ "electricity") in 1880 after observing that a pressure exerted on a small piece of quartz caused an electrical potential between deformed surfaces. Conversely they found that the application of a voltage to a

quartz crystal effects physical distortion (vibrational deformation) of the crystal for a short time until equilibrium is reached.<sup>14</sup>

### Piezoelectric Quartz Crystal Resonators<sup>15</sup>

The piezoelectric effect only occurs in ionic crystalline solids lacking a center of inversion. A crystal structure possessing an accumulated three-dimensional dipole moment of zero will exhibit a new dipole moment if stretched or compressed parallel or perpendicular to the dipole vertices. Similarly, an electric field applied parallel to one of the vertices will cause a distortion of the atoms which results in a contraction or elongation of the crystal parallel to the direction of the field. Of the 32 three-dimensional point groups, 20 possible piezoelectric classes (noncentrosymmetrical) exist. However, some of the crystals belonging to these classes may possess piezoelectric phenomenon too small to detect.

Piezoelectric materials have been used extensively as electromechanical transducers and highly stable oscillators for frequency control. Large piezoelectric coefficients are necessary for the former; mechanical and thermal stability are needed for the latter. Materials with large piezoelectric coefficients include rochelle salt, ammonium dihydrogen phosphate, potassium dihydrogen phosphate, ethylene dihydrogen tartrate, and alpha quartz. Although quartz has the smallest coefficient of the five crystalline substances listed, it also exhibits desirable mechanical and thermal stability properties. It is capable of securing a  $\text{pg/cm}^2$  mass sensitivity, which in principle means that 0.1% of a monolayer of hydrogen is detectable.

Piezoelectric quartz crystal resonators are precisely cut slabs from a single crystal of natural or synthetic quartz. A quartz crystal in its perfect natural form is illustrated in Figure 2.

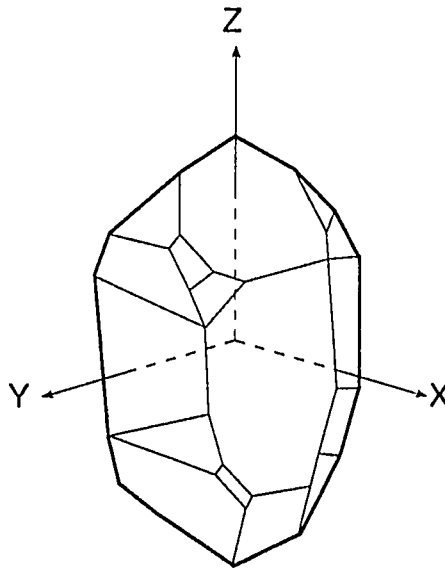


**Figure 2.** A quartz crystal in its perfect natural form as adapted from Lu<sup>14</sup>.

Moderation of the frequency of the driving voltage used to stimulate mechanical vibration produces a quartz crystal oscillator. These devices have been used extensively for time and frequency control applications.

Piezoelectric quartz crystals exhibit many modes of resonance. An example is a rectangular solid bar which exhibits three different types of vibrations: longitudinal (extensional), lateral (flexural and shear), and torsional (twist). Generally it is desirable to have only one principle vibrating mode. This may be accomplished by cutting a quartz crystal slab

at a specific crystallographic orientation which suppresses undesirable modes. Other factors which may influence the mode of resonance include the configuration of the electrodes on the crystal, the supporting structure, and the oscillator circuit.

The high frequency thickness-shear mode is the most desirable mode of vibration since it is most sensitive to the addition or removal of mass for a quartz crystal resonator. The plate motions of the resonator in this mode are essentially one-dimensional (Figure 3).

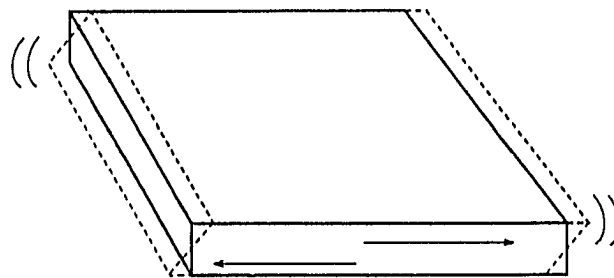


**Figure 3.** The fundamental thickness-shear mode of vibration as adapted from Lu *et al.*<sup>14</sup>

In order to make a quartz crystal plate oscillate in a pure thickness-shear mode, the plates must be cut to a specific orientation with regard to the crystal axes, namely the rotated Y-cut family. AT- and BT- cut crystal plates shown in Figure 4 are representative of singly rotated Y-cuts. Another type of plate, the doubly rotated Y-cut stress compensated (SC) quartz crystal, has been shown to be less sensitive to thermal shock and mechanical stress.

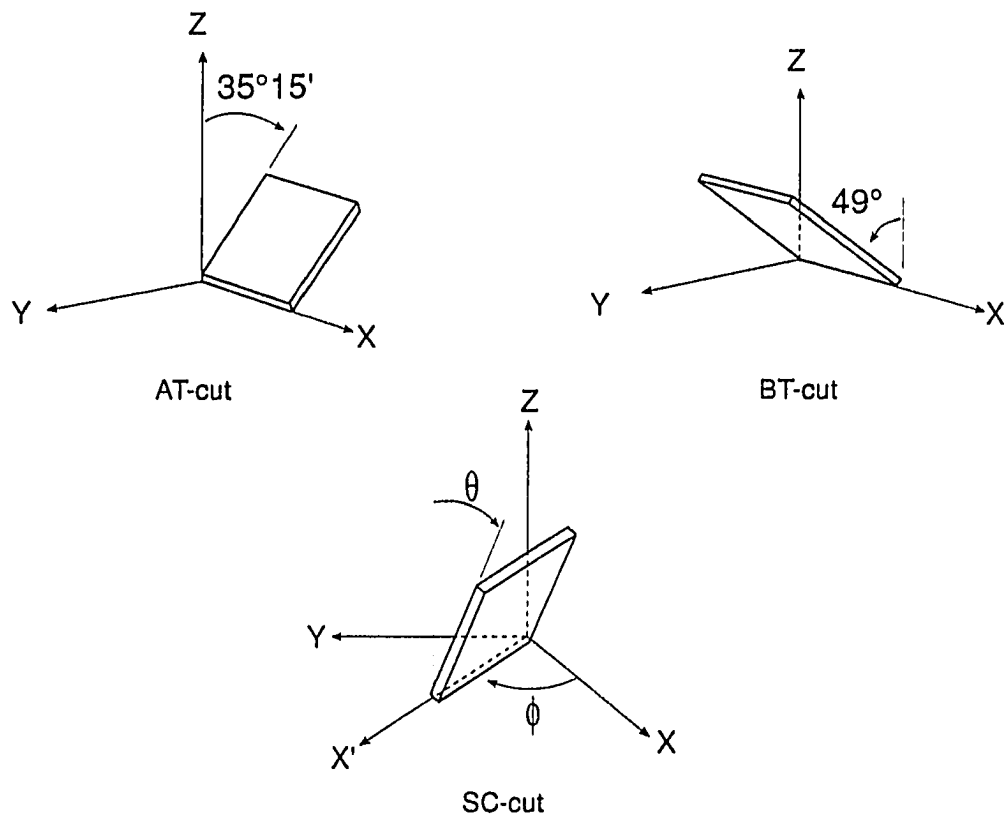


**Figure 4.** AT- cut, BT- cut, and SC- cut (doubly rotated Y-cut) quartz crystal plates as adapted from Lu *et al.*<sup>14</sup>

AT- cut quartz crystal resonate frequencies are insensitive to temperature change in the region around room temperature. It is possible to modify the operating temperature range by changing the standard AT- cut angle of rotation.<sup>16</sup>

For AT- cut crystals, the resonant frequency is inversely proportional to the crystal's thickness and mass sensitivity increases with the square of the frequency. For practical reasons (i.e. difficulty in handling) most research is done using 1-10 MHz crystals.



### Mass Determination by a Quartz Crystal Microbalance

Accuracy of mass measurements is the primary concern in the design and construction of a QCM. Improved accuracy of mass determination is governed by minimizing three factors: 1) errors introduced by the frequency or time measurement technique employed, 2) errors due to resonant frequency changes caused by factors other than mass, such as temperature and stress, 3) the accuracy of the formula used to convert the resonant frequency change to mass. The first factor is an electrical engineering concern beyond the scope of this thesis. The second factor may be minimized by selecting appropriate quartz crystal resonator slab cuts (i.e. AT-, BT- and SC- cuts) by varying crystallographic orientation. The third factor has been addressed by numerous investigators who have attempted to mathematically describe frequency change with respect to mass loading on quartz crystal microbalances.

### General Formulas for Mass Determination by a Quartz Crystal Microbalance

Sauerbrey (1959)<sup>17,18</sup> developed a relationship between the mass of metal films deposited on quartz crystals and the change in frequency. The relationship was derived for quartz (AT-cut) crystals vibrating in the thickness-shear mode:

$$\Delta f = - 2.3 \cdot 10^6 f^2 \Delta m / A$$

where  $\Delta f$  is the change in frequency due to the coating (Hz),  $f$  is the fundamental frequency of the quartz plate (MHz),  $\Delta m$  is the mass of the deposited metal film (g), and  $A$  is the area coated (cm<sup>2</sup>). With regards to

the sensitivity of the device as a mass indicator, this equation predicts that a commercially available 9 MHz crystal would have a mass sensitivity of about 0.4Hz/ng. The detection limit is estimated at about one picogram per square centimeter ( $10^{-12}\text{g/cm}^2$ )<sup>19</sup>. Further investigation and definitions regarding the qualitative nature of how thin films induced resonance phenomenon led to the development of the Sauerbray equation:

$$m_f = -(f_c - f_q)\rho_q v_q / 2f_q^2$$

where  $m_f$  is the mass per unit area of the deposited film,  $f_c$  is the resonant frequency of the quartz crystal with the deposited material,  $\rho_q$  is the density of the quartz crystal,  $v_q$  is the shear wave velocity, and  $f_q$  is the resonant frequency.

Soon after, Stockbridge (1966)<sup>20</sup> developed a perturbation analysis for a one-dimensional vibrating system which describes a mass uniformly distributed over the entire surface of the resonator. This equation assumes that the acoustic wave does not propagate in the film coating. This assumption holds for thin films (~100 nm), but as the mass of deposited material becomes appreciable and forms a uniform layer of finite thickness (~800 nm) the assumption breaks down. Miller and Bolef (1968) took a different approach and treated the combination of the quartz slab and thin film coating as a composite acoustic resonator. In their model, acoustic waves actually propagate into the film. Their equation accounts for the resonance of thick films and can be reduced to Stockbridge's equation for small amounts of added mass. Behrndt and Love (early 1960s) suggested another modified equation to account for perturbations while monitoring film thickness during repeated or extended deposition processes. To further complicate matters, improved QCM designs ( e.g. contoured crystal, edge mounting, and special electrode configurations) have not only

increased the mass loading capabilities, but also the complexity of theoretical explanations. In the general equation suggested by Lu and Lewis (1972), shear modulus and acoustic impedance are addressed. The relationship shows that films with different acoustic impedance, or elastic properties, will obey different mass-frequency relations. For very small mass loads, however, the equation reduces to the Sauerbray equation shown above.

### Design Considerations

When mounting a quartz crystal resonator, the mounting assembly must be designed independently of the resonator ensemble. Also the geometry and size of the electrode and crystal determine the area of maximum sensitivity on the QCM crystal as well as contribute to the suppression of unwanted vibrational modes. The QCMs used in this study were obtained commercially and are of the cemented lead type shown in Figure 5. They have gold electrodes deposited on silicon coated 10 MHz AT- cut quartz crystal resonators.

### **Solid/Vapor Interactions**

Understanding solid/vapor interactions is critical to the design of sensor recognition coatings. This section provides the background for correlating various parameters in molecular modeling of target analytes interactions with sensor coatings.

Sorption interactions between solid phase supports and vaporous analytes have been studied extensively. Early on, the utility of these interactions was recognized as beneficial to researchers in the field of

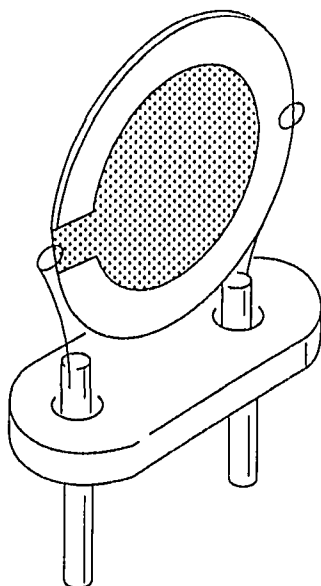


**Figure 5.** Typical cemented lead type 10 MHz AT- cut silicon coated quartz crystal microbalance with gold electrodes.

separation science, in particular, gas-liquid chromatography (GLC). Until around 1990, the most widely used method for classification of GLC stationary phases was one developed by Rohrschneider<sup>21</sup> and subsequently modified by McReynolds<sup>22</sup>. In essence, the method involves the use of a retention index (Kovats retention indices<sup>23</sup>) for a solute on a given stationary phase at a given temperature using a standard set of compounds. An overall stationary phase polarity can be calculated as the sum of the differences of the retention indices of the standard compounds.

### Gas-Liquid Chromatography

Observations of the adsorption of gases on various materials began the initial work in the area of gas chromatography (GC) with the help of the pioneering efforts by Martin and Synge on partition chromatography.<sup>24</sup> A method was developed for separating acetylated amino acids according to their distribution ratio and partition coefficients between a counter current of water and chloroform. They soon discovered that the acetylated amino acids could be separated according to partition coefficients using a chromatographic column filled with silica gel particles with water retained on the silica gel, through which chloroform flowed. This system marked the beginning of partition chromatography. It was further found that by replacing the silica with cellulose the need to derivatize the amino acids was eliminated<sup>25</sup>. Both Martin and Synge were awarded the Nobel Prize in 1952 for this work. Soon after, Martin, with coworker James, developed and refined this earlier work by utilizing nitrogen gas instead of a liquid for the mobile phase. With this technique they were able to separate C<sub>2</sub>-C<sub>4</sub> fatty acids using a stearic acid stationary phase on a celite support<sup>26</sup>. This work led to the development of gas-liquid chromatography (GLC), a technique that has revolutionized analytical chemistry; and which, by 1956, became a widely used routine analytical technique.

### Partition Coefficient

Solute molecule equilibrium distribution between the mobile and stationary phases determines the relative affinity towards each phase and may be viewed in terms of retention characteristics. A partition ratio,

defined as the relative amount of solute in each phase, is described by the partition coefficient  $K$ :

$$K = C_s / C_m$$

$C_m$  is the concentration in the mobile phase and  $C_s$  is the concentration in the stationary phase. The partition coefficient is related to the standard Gibb's free energy of solution of a gaseous solute<sup>27</sup>,  $\Delta G_s^\circ$ , by:

$$\Delta G_s^\circ = -RT \ln K$$

The frequency shifts due to vapor sorption into coatings of piezoelectric chemical mass sensors is directly related to the partition coefficient<sup>28,29,30,31</sup>. A simple relationship which relates frequency shift,  $\Delta f_v$ , caused by vapor sorption to the partition coefficient and experimentally determined sensor characteristics for QCM delay lines is as follows<sup>8</sup>:

$$\Delta f_v = \Delta f_s C_v K / \rho$$

Where  $\rho$  is the density of the coating material,  $C_v$  is the vapor concentration, and  $\Delta f_s$  represents the frequency shift observed after a coating is applied to an uncoated QCM device.

### Factors that Influence Retention

There are numerous molecular interactions that determine how a component will be distributed between mobile and stationary phases. These interactions may be oriented or non-oriented. They involve combinations of polar forces which arise from induced and permanent electric fields (dipole/dipole, dipole/induced-dipole, induced-dipole/induced-dipole) and London's dispersion forces. The latter are influenced by the relative molar masses of the solute and solvent<sup>32</sup>. In this

case, hydrogen bonding is considered a polar force. Several inter-molecular forces predominate but polar and dispersion forces account for the major contributions to the overall interactions. The relative polarities of solvents are often quoted as the dielectric constants in GLC, however for chemical mass sensors, subtle distinctions regarding dipolarity and polarizability need to be considered.

### Choice of Stationary Phase

Solute retention volumes and retention times are characteristically used to determine stationary phase selection. Various retention index methods exist for evaluating the partition and separation properties of solute-stationary phase systems.

Kovat's retention indices<sup>33</sup> (KRI) are frequently used to indicate the chromatographic retention properties of a column with respect to the *n*-alkanes. The *n*-alkanes are used as reference materials since they are chemically inert, soluble in most common stationary phases, and are defined as having a  $KRI = 100 \times n$  (*n* being the number of carbons present in the molecule.) e.g. *n*-hexane = 600 and *n*-octane = 800 regardless of the column used or the operating conditions. (These species are recorded individually for each column.)

A graph of  $\ln(RT)$  against retention index is constructed for several alkanes. The KRI for other compounds to be investigated is determined by recording retention indexes (RI) and reading the RI of the graph. For example, propanol may have an RI of 650 on a Carbowax column, but only 500 on a OV101 column. This implies that the Carbowax is the more

polar column by 150 RI units. Kovat's indices may be calculated from the equation,

$$I = 100[(\log V^u - \log V^x) / (\log V^{x+1} - \log V^x)]$$

where  $V$  is the retention time of the compound denoted by the superscript,  $x$  is the carbon number of the alkane eluted before the unknown,  $(x+1)$  is the carbon number of the alkane eluted after the unknown,  $u$  refers to the unknown. This formula is based on the linear relationship between  $\log V$  (retention volume) and carbon number for a homologous series. A more general expression is given by:

$$I = 100[n\{(\log V^n - \log V^x) / (\log V^{x+n} - \log V^x)\} + x]$$

The terms are the same as the previous equation. In addition,  $n$  refers to the difference in the number of carbon atoms for the  $n$ -alkanes used as reference.

Rohrschneider<sup>34</sup> and McReynolds<sup>35</sup> extended the RI system comparing the RI for the  $n$ -alkanes on the given column with those on a squalane column. The difference in RI values gives the solute/stationary phase interactions due to hydrogen bonding, dipole moment, and acid-base properties since these will be over and above the squalane non-polar interaction. The method is useful for column selection where components have different functional groups, and for identifying stationary phases with similar properties.

Some difficulties are associated with the Rohrschneider-McReynolds method. Pool *et al.*<sup>36</sup> criticize the method on both technical and theoretical grounds. The primary technical objection being that alkanes (necessary for the determination of  $I$  values) are sorbed onto polar stationary phases mainly by interfacial adsorption, rather than by true gas-liquid partitioning. If the  $I_p$  values are incorrect, then the whole procedure



is invalid (for polar phases). A theoretical objection is that the 'overall polarity', cannot be a true measure of polarity, since it depends principally on solubility of the *n*-alkanes in the stationary phase. There are other difficulties associated with the Rohrschneider-McReynolds method. The method is entirely restricted to GLC retention data so there is no possibility of comparing GLC stationary phases with common solvents. Secondly, the method is far too coarse to allow any analysis of solute-solvent interactions, which are actually the basis of gas-liquid partition, hence of retention data.

#### Linear Solvation Energy Relationships

Abraham *et al.*<sup>37</sup> have developed the Linear Solvation Energy Relationships (LSER) system for characterizing interactions that occur with GLC stationary phases, common solvents, and any condensed phases. The LSER system has also proven useful in describing analyte vapor interactions with chemically coated mass sensors<sup>4</sup>. The method utilizes one of the most extensive and carefully determined sets of data compiled by Laffort *et al.*<sup>38</sup> listing retention indices of 240 compounds on five stationary phases at 393 K. In addition, the method introduces descriptors for both acidic and basic hydrogen bonding and cavitation in solute/stationary interactions.

Abraham, Doherty, Kamlet, and Taft<sup>28</sup> suggest the following equation to incorporate the parameters:

$$\text{Log } K' = c + rR_2 + s\pi_2^* + a\alpha_2H + b\beta_2H + l\text{Log } L^{16}$$

$K'$  is a modified gas-liquid partition coefficient,  $c$  is a constant,  $rR_2$  is the solute polarizability,  $s\pi_2^*$  is the solute dipolarity,  $a\alpha_2H$  is the solute hydrogen-bond acidity,  $b\beta_2H$  is the solute hydrogen-bond basicity,  $l\log L^{16}$  is a term which relates dispersion forces and cavity effects. (Note: The subscripted "2" denotes solute or analyte, whereas a subscripted "1" would denote stationary phase or coating.)

### Polarizability

"Polarization is the readjustment of a charge distribution when it experiences a static external electrical potential. Instead of the word "polarization," the term "induction" is often used for this effect on charge distribution. When both terms are used, induction is usually reserved for molecular level effects and polarization for macroscopic effects." .....<sup>39</sup>

"A dipole is *induced* by an external field ...because the charge distribution has been *polarized*. The dipole moment, the dipole polarizability, and the dipole hyperpolarizability are 1st, 2nd, and 3rd derivatives of the energy with respect to the field strength, respectively. Polarization incorporates cooperative or nonpairwise additive elements into a potential." For example, in a system of three molecules, A, B, and C, the polarization energy is the sum of contributions from each molecule. In essence, the formation of a dipole in a structural unit or non-dipolar molecule when exposed to an electric field is referred to as polarizability. For example, the presence of aromatic groups or heavy halogen atoms in a compound exhibit this property by providing polarizable  $n$  and  $\pi$  electrons.

### Dipolarity

Dipolarity is a term used to describe oriented dipole-dipole interactions. Molecules that have permanent dipoles tend to associate more strongly with one another than to non-polar molecules. Dipole-induced dipole interactions also increase vapor sorption interactions via polarizability effects. In either case, only components with similar dipoles will disperse in the solvent and produce solute-solvent pairs.

### Hydrogen Bonding

Hydrogen bonding describes the interaction that occurs when an  $H^+$  accommodates to electron pair clouds in order to bind to polar molecules.<sup>40</sup> The force of these bonds is weak (10 to 40 kJ). The location of the hydrogen bonds occur at a preferred molecular orientation, in particular, where the shared hydrogen forms the vertex of the angle ( $\sim 120$ - $240^\circ$ ) between the polar substituents. Hydrogen bonding may be classified as either acidic or basic depending on whether the substituent is donating or receiving the shared hydrogen, respectively. The most common examples of acidic hydrogen bonding compounds are alcohols and phenols which possess an OH group; however, NH groups can also be acidic. The addition of electron-withdrawing halogen substituents can greatly enhance the acidity of hydroxyl groups. Fluoropolyol is one type of mass sensor coating which exploits this property. Some basic hydrogen bonding compounds include tertiary, secondary, and primary aliphatic amines. Tertiary amines are stronger hydrogen-bond bases because they contain no NH groups like primary and secondary amines which have a tendency to self-association. Poly(ethylenimine)  $-(CH_2CH_2NH)-$  is an example of a hydrogen-bond base coating that possesses secondary amine functionality

and is sensitive to hydrogen bond acids. Some amphiprotic compounds such as water and acetic acid may possess both acidic and basic hydrogen bonding properties. Acetic acid can also readily self associate to form a strongly bound dimer.

### London Dispersion Forces

Dispersion interactions, also known as London dispersion forces and as instantaneous-dipole/induced-dipole interactions are characteristically described as weak attractive forces (10-40 kJ/mole) between atoms and molecules. Aliphatic hydrocarbons in the condensed phase epitomize these forces which may be viewed as oscillating charges that produce synchronized dipoles that attract each other. Increasing the length of an aliphatic chain increases the potential for dispersion interactions. The sum of such interactions can be quite significant and can explain why *n*-pentane, a small molecule, is a liquid at room temperature, and why hexadecane boils at 287 °C and solidifies at 18 °C . Both exhibit entirely dispersive interactions. Poly(isobutylene) is an example of a sensor coating material which exhibits only dispersion forces. Poly(isoprene) and poly(butadiene) are examples of unsaturated elastomeric aliphatic polymers that exhibit similar dispersion sorption interactions when used as coatings; they are however, subject to degradation by ozone.<sup>41</sup>

### Cavity Effects

Cavity effects describe the cavity formation and closure processes which occur when a solute (analyte) molecule is sorbed into a solvent

(solid phase) . Cavity effects tend to increase as the solvent cohesive energy density increases. That is, if solvent molecules adhere to one another tightly, it is more difficult to separate them than if they adhere lightly. Increases in cavity effects contribute to a decrease in the  $l$ -coefficient. (See the LSER equation.) The combined effects of dispersive forces and cavity effects on the  $l$ -coefficient influences the solubility of gaseous components. The larger the value of  $l$ , the larger the difference in the partition coefficient.

## Sorption Isotherms

### General

Sorbition of analytes onto recognition coatings is a complicated process which could involve several phenomena. This section briefly describes relevant aspects of adsorption isotherms.

Gases sorb onto solid surfaces from valence force attractions that arise from unsaturated atoms and molecules on the surface. The amount of adsorption which occurs between a gas and a stationary phase can be described as a function of the equilibrium pressure of the gas at a fixed temperature. If a known amount of gas is introduced into an evacuated chamber containing a solid adsorbent, the amount of gas adsorbed may be determined by measuring the pressure and volume of the remaining gas at equilibrium.

The forces which contribute to adsorption are usually classified as either *physical adsorption* or *chemisorption*. Physical adsorption describes gas/solid non bonding interactions that occur, such as London

forces and dipole forces. In this case, hydrogen bonding is considered a dipolar force. Chemisorption describes chemical bond formation energy; it is much greater than physical adsorption.

### Monolayer Adsorption - The Langmuir Isotherm

Sometimes an adsorption isotherm may indicate that the surface is saturated at high pressures. In 1918 Irving Langmuir<sup>42</sup> derived an equation based on the kinetic model which describes equilibrium in terms of a fraction of the fixed number of adsorption sites occupied on a surface with respect to adsorption or desorption of gas. Later Fowler and Guggenheim<sup>43</sup> developed a statistical thermodynamic model in which gas molecules are adsorbed on uniform fixed sites of the surface. Their work indicated that "the form of the Langmuir isotherm does not depend on any assumptions about the kinetics of adsorption and desorption; it depends only on the assumptions that the gas is adsorbed to fixed sites and that the adsorbed molecules do not interact with one another."<sup>44</sup>

### Multilayer Adsorption -The Brunauer- Emmet-Teller (BET) Isotherm

Often it is necessary to view molecular adsorption over a surface in terms of successive layers rather than a single monolayer. Brunauer, Emmet, and Teller<sup>45</sup> were the first to propose a modification of the Langmuir isotherm to account for multilayer adsorption. According to Hill<sup>46</sup>, the physical model on which the BET equation is based requires several assumptions:

1. The surface of the solid adsorbent contain a uniform single layer of a fixed number of adsorption sites which are equivalent.
2. Molecules adsorbed to the first layer are localized; i.e. they are each fixed to an individual adsorption site and are not free to move around.
3. The first layer of gas molecules provide sites of adsorption for the second layer of gas molecules which provide sites for the third layer of gas molecules and so on. There is no limit to the number of possible layers.
4. In any given layer there is no interaction between the molecules. The layers are viewed as independent stacks of molecules built upon the surface sites.
5. Molecules in the first layer, those in direct contact with adsorption sites, have higher energy of interaction than molecules in the higher layers. The higher layer molecules eventually take on the energy characteristics of the bulk phase.

The equation may also be derived using a statistical mechanics model based on equilibrium considerations. The BET isotherm derived using either the physical (kinetic) model of the statistical mechanics model is as follows<sup>47</sup>.

$$\theta = \frac{n}{S} = \frac{cx}{(1-x)[1+(c-1)x]}$$

$\theta$  is the ratio of adsorbed molecules to available sites,  $S$  is the number of sites,  $n$  is the number of adsorbed molecules,  $x$  is the relative pressure ( $p$  (the partial pressure divided by the dilution factor) divided by  $p_0$  (the partial pressure) or  $p/p_0$ ), and  $c$  is a dimensionless constant. Note that

coverage approaches zero as the relative partial pressure approaches zero. Also, the coverage approaches unity as the relative partial pressure approaches infinity. If the adsorbed volume required to cover the entire surface with a monolayer is denoted by  $v_m$ , one can describe the isotherm in terms of the coverage  $\theta$ :

$$\theta = \frac{v}{v_m}$$

This rearrangement provides the usual form of the BET equation:

$$\frac{x}{v(1-x)} = \frac{1}{v_m c} + \frac{(c-1)x}{v_m c}$$

A plot of  $[x / v(1-x)]$  versus  $x$  should yield a straight line, however deviations are often observed below  $x = 0.05$  or above  $x = 0.3$ . Both the monolayer volume  $v_m$  and the constant  $c$  can be evaluated from the slope and intercept of the plot.



## Chapter 2

### **OBJECTIVES AND HYPOTHESIS**

#### **Objectives**

The objective of this research was to assist in the technology development and design of a chemical vapor detector system based on emerging chemical microsensor and microinstrument technology. Chemical mass sensors including Quartz Crystal Microbalances (QCM) and Surface Wave Acoustic (SAW) devices were employed.

Specific aspects of this work included performing molecular modeling studies involving candidate recognition coatings and various organic analytes of drug interdiction. Our interest was to obtain the best fit for molecular association to optimize both selectivity and sensitivity. This information is considered important for identifying and synthesizing candidate coatings. An additional objective was to evaluate selected candidate coatings and compare the findings with theoretical results obtained from molecular modeling methods.

#### **Hypothesis**

Molecular modeling methods may prove useful in designing and selecting chemical recognition coatings for mass sensor devices by

providing information regarding the sensitivity, selectivity and other aspects of solid/vapor interactions. Practitioners have not utilized molecular modeling methods for this purpose previously.

## Chapter 3

### **EXPERIMENTAL**

#### **Methods and Materials**

##### Materials and Equipment

Poly(ethylenimine) was obtained from Scientific Polymer Products, Inc., Ontario, NY. Formic, propanoic, butanoic, pentanoic, and hexanoic acids were obtained from Aldrich Chemical Company, Milwaukee, WI; acetic acid, sodium hydroxide, and phenolphthalein from J. T. Baker, Inc., Union City, CA and potassium acid phthalate (0.05N) from LabChem Inc., Pittsburgh, PA. Nanopure water was processed in a Barnstead Nanopure Water System. Nitrogen (99.998% purity) was obtained from Airco, Las Vegas, NV.

Uncoated QCMs (10MHz) with gold-surface electrodes were obtained from Universal Sensors, Metairie, LA. Microsensor Systems, Inc., Bowling Green, KY supplied the QCM devices (158 MHz), the vapor generator (Model VG-400) and the frequency counter (Model DAS 158). An Apple® Macintosh Classic microcomputer was used to process the data using mass sensor software supplied by Microsensor Systems, Inc.

The vapor generator utilized for corrosive vapors was custom designed.<sup>48</sup> The unit is made from 1/4" stainless steel valves and tubing. The valves may be adjusted to control the flow of carrier gas and vapors such that they dilute and mix prior to reaching the surface of the mass sensor device. (See Figure 6.)

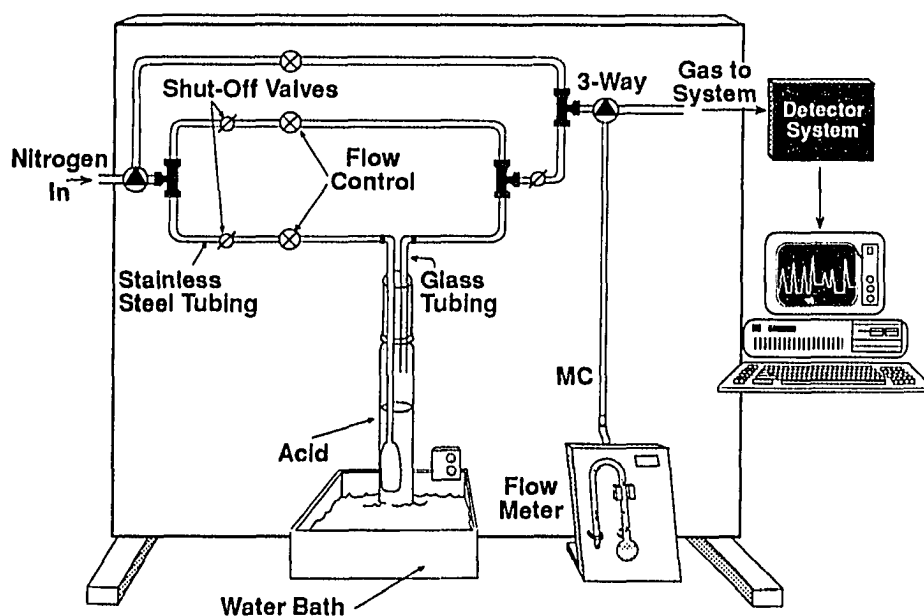


**Figure 6.** Corrosive vapor generator designed and built by Dominguez, Lin, and Li.<sup>49</sup>

### Vapor Generator Calibration

Two distinct methods were employed for calibrating the vapor generators. The first method, activated carbon adsorption, involved collecting vapors in a preweighed syringe filled with activated charcoal for

a set amount of time (usually 30 min)<sup>49</sup>. The syringe was reweighed in an analytical balance to determine the mass of vapors absorbed. The measurement was repeated in triplicate and the average and percent relative standard deviation were calculated. For acidic vapors a second method was employed. The acidic vapors were bubbled into a flask containing methanol and titrated with a standardized sodium hydroxide solution ( $\sim 0.01\text{N}$ ) using phenolphthalein as an indicator. The sodium hydroxide solution was standardized using potassium acid phthalate.

## **Recognition Coating Study**

### Film Thickness and Sensitivity

A 0.1 % PEI solution (0.2 g of 50% PEI in water in 100 mL of methanol) was successively drop coated ( $0.5\text{ }\mu\text{L/drop}$ ) on five 10 MHz QCM sensors and allowed to evaporate until thicknesses of 0.69, 0.76, 1.7, 4.1,  $4.4 \pm 0.1\text{ KHz}$  were obtained. Generally, for a coated piezoelectric mass sensor, the coating thickness is defined as a measure of frequency change and is expressed in Hertz (cycles per second). Coatings vary greatly in density, elasticity, and coverage. For practical purposes, a four Hz frequency change equates (approximately) to a 1 nm coating thickness.<sup>50</sup>

The corrosion resistant vapor generator was used to administer acid vapors to the QCM sensor. Approximately 150 mL of each acid was poured into the vapor generator bubbler flask and allowed to equilibrate to the water bath temperature of  $20.0 \pm 0.3\text{ }^{\circ}\text{C}$ . The QCM sensor was maintained at room temperature,  $20 \pm 3\text{ }^{\circ}\text{C}$ .

The nitrogen carrier gas flow was set to 100 cc/min. Neat acid vapors were introduced to the QCM sensor in alternating pulses of 40 s intervals. Between pulses, nitrogen was introduced for 40 s to purge the sensor surface. After each run (series of pulses) the sensor response was allowed to equilibrate to the original baseline. A typical QCM response curve is shown in Figure 7. The frequency change (QCM response) was determined by subtracting the average of the peak minima from the average of the peak maxima for four sets of peaks.

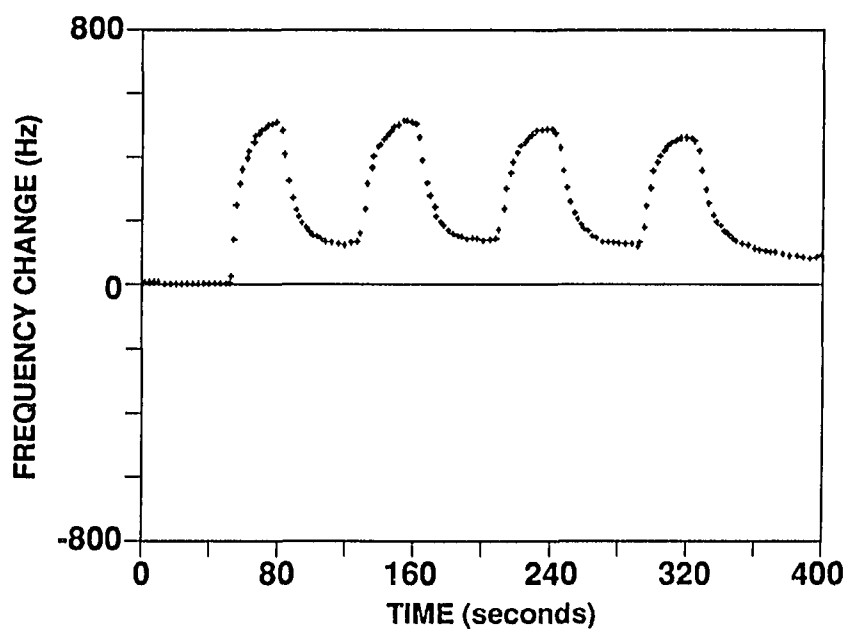


**Figure 7.** A typical 10 MHz QCM frequency response curve showing the baseline and introduction of alternating 40 second pulses of benzoic acid vapors and nitrogen purge.

Since the vapor pressures of the individual acids vary significantly, it was necessary to mathematically correct the frequency responses to account for the numbers of molecules available for interaction with the coated QCM sensor surface. For instance, the vapor pressure of acetic acid is 11.4 mm Hg at 20 °C and butanoic acid is 0.43 mm Hg at 20 °C. For neat solutions (equal dilutions of the acids), a higher QCM response is observed for acetic acid than for butanoic acid due to the large number of acetic acid molecules coming in contact with the coated QCM surface. After vapor pressure corrections, the butanoic acid exhibits the higher sensitivity.

## **Analyte Studies**

### **Isotherm Determination**

A 10 MHz QCM was drop coated (0.5 $\mu$ L/drop) until a desired mass of  $2.0 \pm 0.1$  KHz was obtained. Eight dilutions each (20.0 x, 10.00 x, 5.00 x, 3.33 x, 2.00 x, 1.43 x, 1.25 x, and  $1.00 \pm 0.05$  x) of formic, acetic, propanoic, butanoic, pentanoic, and hexanoic acids were used. Utilizing the corrosion resistant vapor generator previously described, dilutions were accomplished by adjusting the flow rate of the acidic vapors with respect to the flow rate of the carrier gas (nitrogen). The ratios of acidic vapor flow rates (cc/min) to nitrogen flow rates (cc/min) were 5/95, 10/90, 20/80, 30/70, 50/50, 70/30, 80/20, and 100/0, respectively for the dilutions listed above. After purging the QCM sensor surface with nitrogen for 40 s, dilute acid vapors were introduced to the QCM for approximately 460 s continuously or until a horizontal peak maximum

absorbance was observed. Nitrogen was then introduced (usually 500 s) to purge the sensor surface and allow the sensor response to return close to the original baseline. The overall frequency change was calculated as the difference between the average peak maxima and average baseline minima. The final frequencies were corrected for analyte vapor pressure differences.

#### Dilution Effects and Coating Sensitivity

Calculations and analyses were performed using data obtained above for six dilutions (20.0 x, 5.00 x, 2.00 x, 1.43 x, 1.25 x, and 1.00 x  $\pm$  0.05 x) of formic, acetic, propanoic, butanoic, pentanoic, and hexanoic acids using the 2.0 KHz PEI coated QCM.



## Chapter 4

### RESULTS AND DISCUSSION

#### Recognition Coating Studies

##### Film Thickness and Sensitivity

The purpose of this study was to determine whether varying thicknesses of poly(ethylenimine) (PEI) coating on a QCM would produce a linear response when exposed to the individual vapors of a homologous series of carboxylic acid vapors. (The Sauerbrey equation infers a linear response.) Another purpose was to determine the relative sensitivity of the PEI coating for each of the vapors. As mentioned in the hydrogen bonding section in chapter 4, PEI is capable of forming hydrogen bonds with the hydrogen-bond acids. Amines and carboxylic acids are also capable of forming ionic bonds, especially in solutions. However, hydrogen bonding appears to dominate when low analyte concentrations compete for a large number of binding sites. The reversibility of the vapor/solid interactions support this. Comparison of the LSER values for acetic, propanoic, and butanoic acids, all capable of acidic hydrogen bonding, and to a lesser extent basic hydrogen bonding, suggests that sensitivity (frequency change) to the PEI coating should increase with increasing aliphatic chain length. The data in Table 2 indicate that acid analyte LSER values with

respect to dipolarity ( $\pi_2^*$ ) and hydrogen bonding ( $\alpha_2^H$  and  $\beta_2^H$ ) differ by very little between the acids. The LSER values further indicate that the addition of subsequent methylene groups ( $-\text{CH}_2-$ ) may decrease the polarizability ( $R_2$ ) slightly for each acid, however methylene addition also significantly increases the dispersion interactions ( $\log L^{16}$ ) which can occur. PEI is a non-polarizing coating so analyte polarizability interactions should be minimal.

**Table 2.**

LSER values for a homologous series of carboxylic acids as adapted from Abraham *et al.*<sup>38</sup>

Acid	$R_2$	$\pi_2^*$	$\alpha_2^H$	$\beta_2^H$	$\log L^{16}$
formic	NA	NA	NA	NA	NA
acetic	.265	.60	.55	.43	1.750
propanoic	.233	.60	.54	.43	2.290
butanoic	.210	.60	.54	.42	2.830
pentanoic	.205	.60	.54	.41	3.380
hexanoic	.174	.60	.54	.39	3.920
heptanoic	.149	.60	.54	.38	4.460
octanoic	.150	.60	.54	.36	5.000

NA = Not Available

It was anticipated that coating thickness versus frequency change would produce a linear response for each acid; and the slopes of the linear plots should increase with increasing chain length. Furthermore, it was determined that semi-empirical calculations of van der Waals' force contributions should be roughly correlated with the experimentally determined LSER dispersion values less polarizability values (slopes of

lines) and should predict trendwise the acid sensitivities to the PEI coating. Graphic representations of the results are illustrated in Figures 7 and 8.

Figure 8 illustrates that the plots of coating thickness versus frequency change for each of the acid analytes yielded straight lines with linear regression values ( $R^2$ ) for acetic, propanoic, butanoic, and pentanoic acids of 0.993, 0.898, 0.996, 0.998, respectively, using five observations and three degrees of freedom for each acid. (The standard error of Y estimate ranged from  $\sim 33$  to 422, and the standard error of the X coefficient ranged from  $\sim 9$  to 117, respectively.) The plots further indicate that the sensitivity of the PEI coating increased with increasing aliphatic chain length such that the order of sensitivity was acetic < propanoic < butanoic < pentanoic.

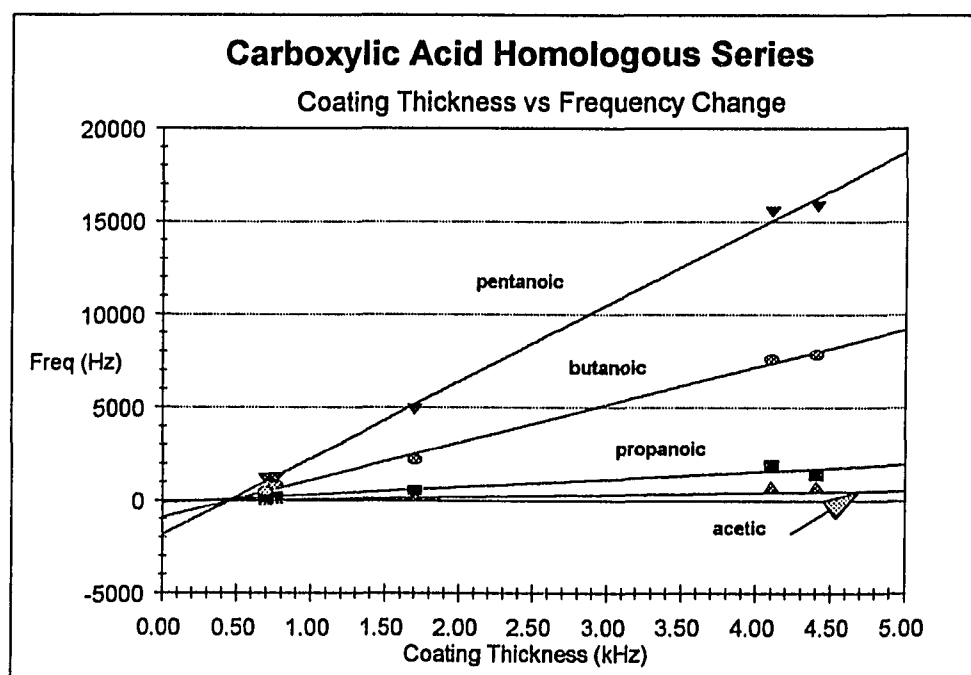


**Figure 8.** Poly(ethylenimine) coating thickness versus frequency response for a homologous series of carboxylic acids using a 10MHz QCM.

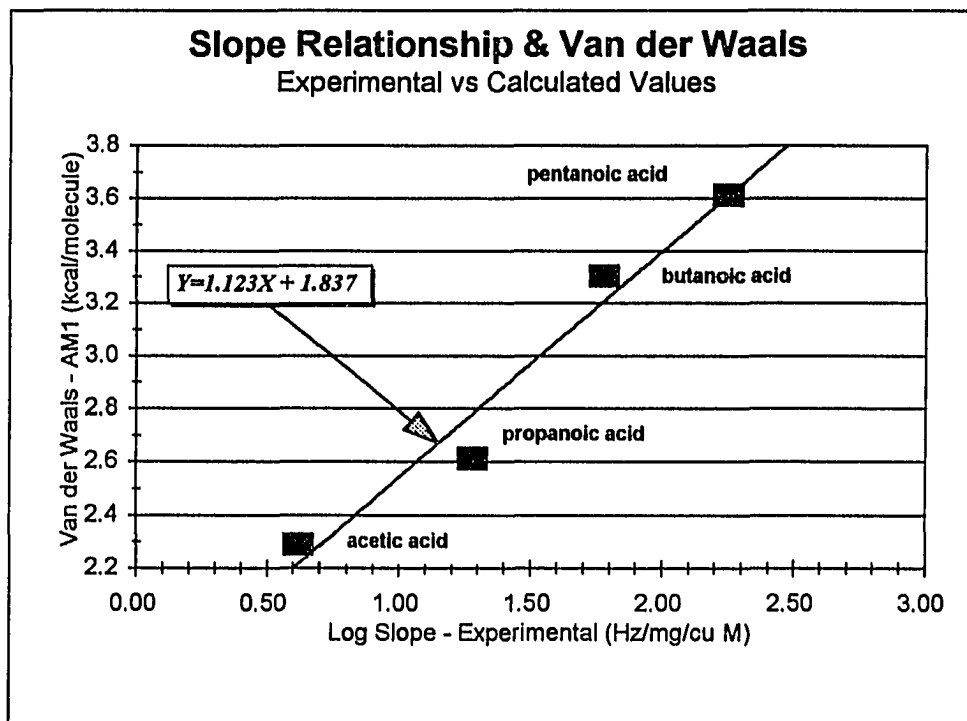


**Figure 9.** Relationship of experimentally obtained dispersion force slope values versus calculated van der Waals force values for a homologous series of carboxylic acids. (Decreasing polarizability force values are also included in the dispersion force values for increasing aliphatic lengths which may or may not be negligible.)

PCModel semiempirical software was utilized to calculate van der Waals (vdW) forces for each of the acid analytes after a molecular structure optimization using the Unrestricted Hartree-Fock (UHF) method was obtained. (There is some discrepancy whether these force values truly represent dispersion forces or the capacity to form vdW bonds. The literature which accompanies the software does not provide a comprehensive explanation of the force value. The values increase as aliphatic chain length increases.) The attractive vdW values for acetic,

propanoic, butanoic, and pentanoic acids were 0.62, 1.28, 1.78, and 2.25 kcal/molecule, respectively indicating that dispersive interactions increase with increasing aliphatic chain length. The vdW values were plotted against the log of the slope values obtained from the regression equations for the individual acid analytes. The plot (Figure 9) suggests a linear relationship may exist. A linear regression coefficient ( $R^2$ ) of 0.962 was obtained. The regression equation  $Y = 1.123X - 1.837$  from four observations and two degrees of freedom indicates a standard error of Y estimate and X coefficient of 0.167 and 0.159. These results suggest that molecular modeling using semiempirical methods may be used to predict trendwise the sensitivity of a coating to analytes with similar functional groups that differ mainly by dispersive interactions.

## Analyte Studies

### Isotherm Determination

Isotherm studies using formic, acetic, propanoic, and butanoic acids, a homologous series, were performed to determine the energy of absorption between the solid phase and the analytes and to discern whether physical adsorption or chemisorption processes occurred. Figure 10 illustrates a typical isotherm measurement using a 2.0 KHz PEI coated 10 MHz QCM sensor. Since reversibility (both sorption and desorption) were observed, it was thought that physical adsorption was involved.

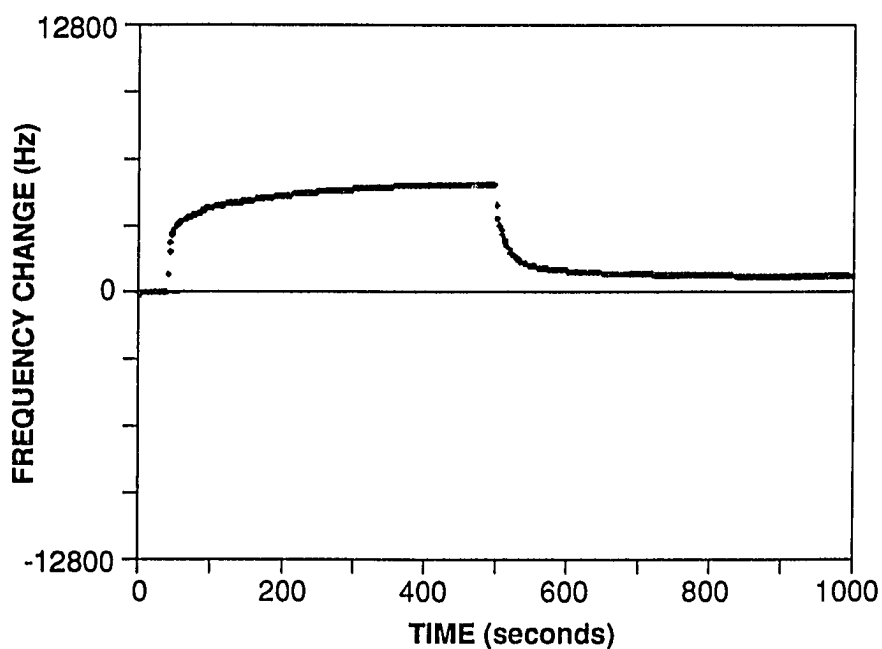


**Figure 10.** Typical isotherm of poly(ethylenimine) coated 10 MHz QCM frequency response to acetic acid vapors.

Figures 11 through 14 illustrate the isotherm plots for the interactions of each acid at several concentrations. The sensitivity of sensor frequency response varies significantly depending on the analyte; a plot combining all the isotherms is shown in Figure 15. The concentration units are expressed in milligrams per cubic meter. These units are characteristically reported for mass sensor measurements probably because they account for differences in molecular weight, vapor pressure, and signify mass per unit volume (areal density). The S shape of the plots are characteristic type II BET isotherms. The plots show that initially at low concentrations a gradual rise in the slope demonstrates monolayer sorption. After the first layer is filled, multilayer sorption is observed by a steep increase in the slope.

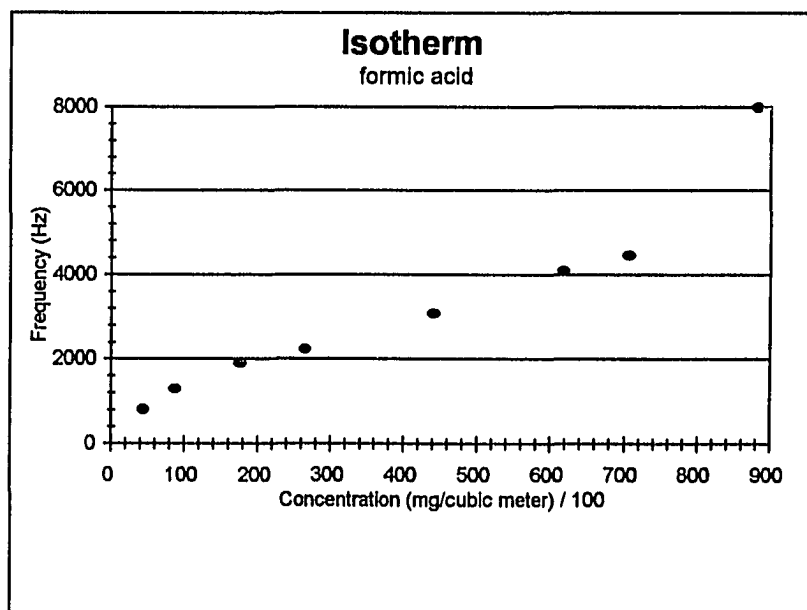


**Figure 11.** Isotherm plot for formic acid interaction with 2.0 KHz PEI coated 10 MHz QCM.

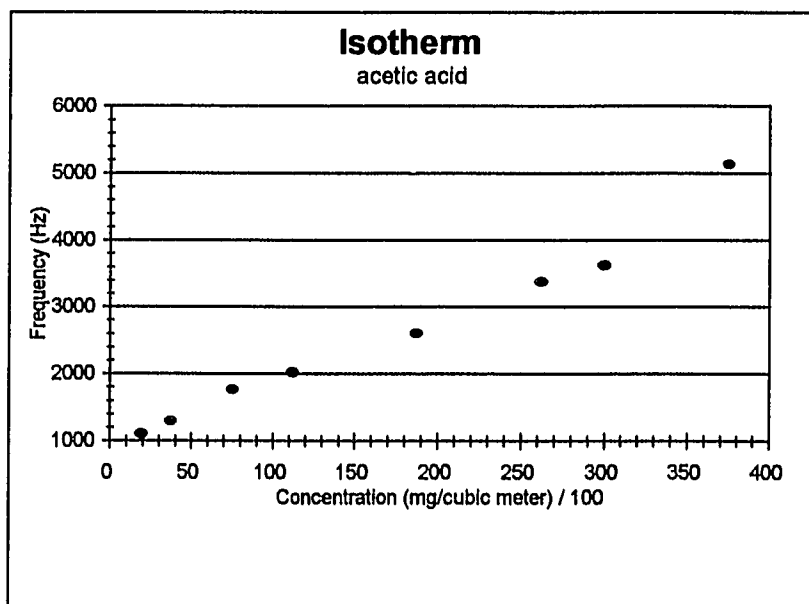


**Figure 12.** Isotherm plot for acetic acid interaction with 2.0 KHz PEI coated 10 MHz QCM.

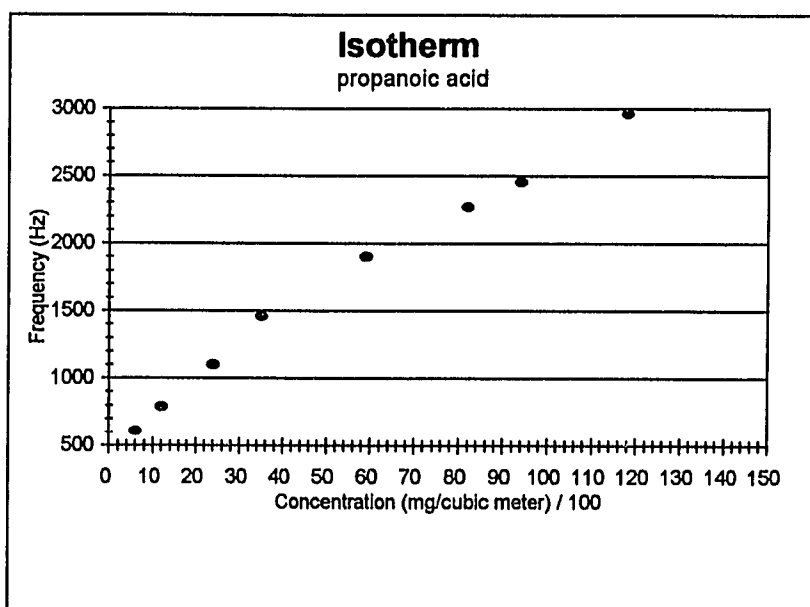


**Figure 13.** Isotherm plot for propanoic acid interaction with 2.0 KHz PEI coated 10 MHz QCM.



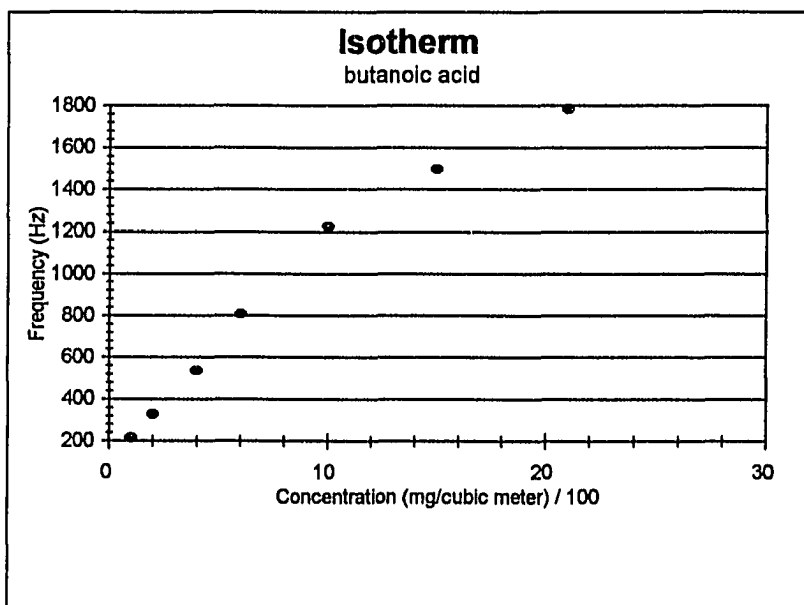


**Figure 14.** Isotherm plot for butanoic acid interaction with 2.0 KHz PEI coated 10 MHz QCM.

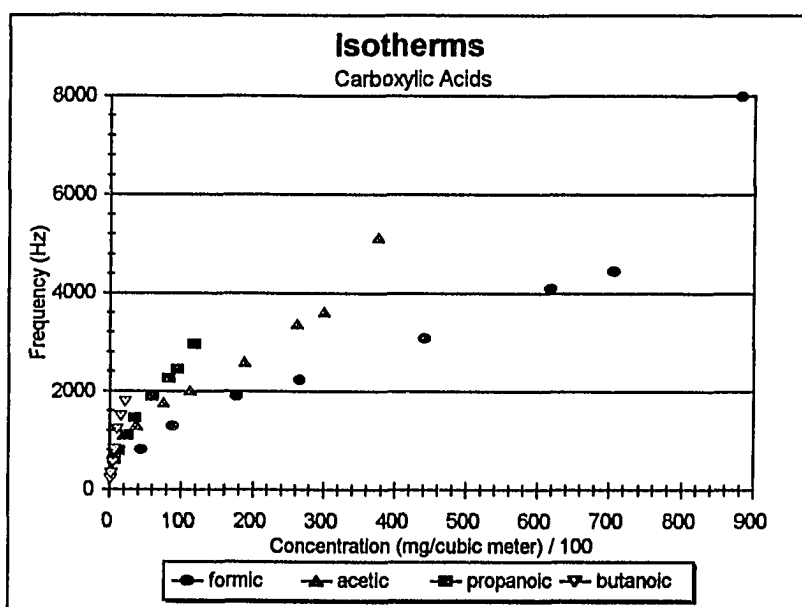


**Figure 15.** Combined isotherm plot for formic, acetic, propanoic, and butanoic acids interactions with 2.0 KHz PEI coated 10 MHz QCM.

The plots were linearized using a Michaelis-Menten like equation. (See Figures 15 through 19) The linear regression coefficients ( $R^2$ ) for formic, acetic, propanoic, and butanoic acids were 0.992, 0.993, 0.991, and 0.988, respectively. The four regressions are included under "Enthalpy Determination" in Appendix I. The standard error of Y estimate ranged from 0.302 to 0.615 and the standard error of the X coefficient ranged from .845 to 1.718 for five observations and three degrees of freedom. Plots of the slopes of the linear portions, 16.266, 17.821, 21.700, and 26.905 for formic through butanoic and solution of the equation  $\Delta H = RT \ln \text{slope}$ , yielded the heats of adsorption for the individual acid analyte vapor interactions with the PEI coating. The calculated heats of adsorption for formic, acetic, propanoic, and butanoic acids were 1.62, 1.68, 1.79, and 1.92 kcal K<sup>-1</sup> mol<sup>-1</sup>, respectively, which indicates that physical adsorption processes occur. For formic through butanoic acids, the differences in heats of adsorption, which are theorized to correspond to dispersive force interactions, were 0.05, 0.11, and 0.12 kcal K<sup>-1</sup> mol<sup>-1</sup>. The lower energy difference associated with formic and acetic acid (0.05 kcal K<sup>-1</sup> mol<sup>-1</sup>) probably occurs because formic acid lacks a methyl group. The differences between acetic and propanoic (0.11 kcal K<sup>-1</sup> mol<sup>-1</sup>), and propanoic and butanoic (0.12 kcal K<sup>-1</sup> mol<sup>-1</sup>) are more equidistantly separated and may correspond to the energy of methylene addition. (See Figure 21.)

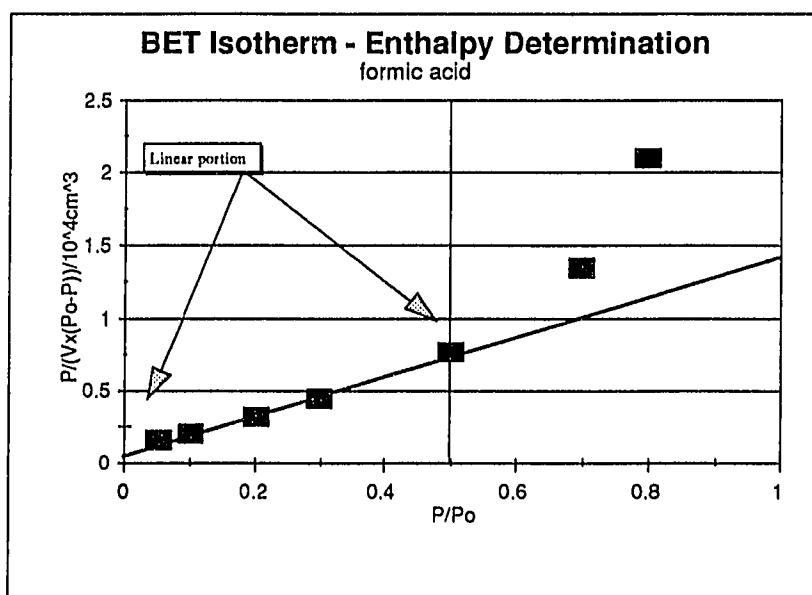


**Figure 16.** Linearized form of BET isotherm for formic acid interaction with 2.0 KHz PEI coated 10 MHz QCM.

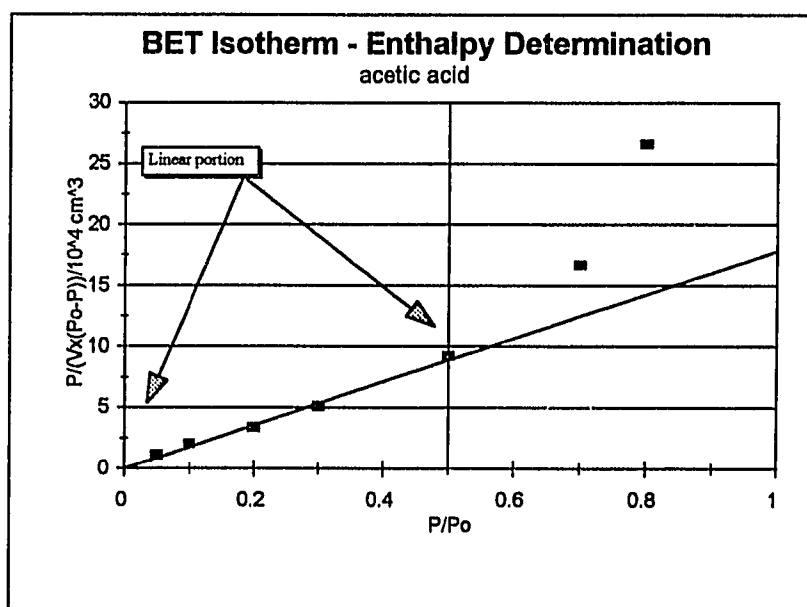


**Figure 17.** Linearized form of BET isotherm for acetic acid interaction with 2.0 KHz PEI coated 10 MHz QCM.

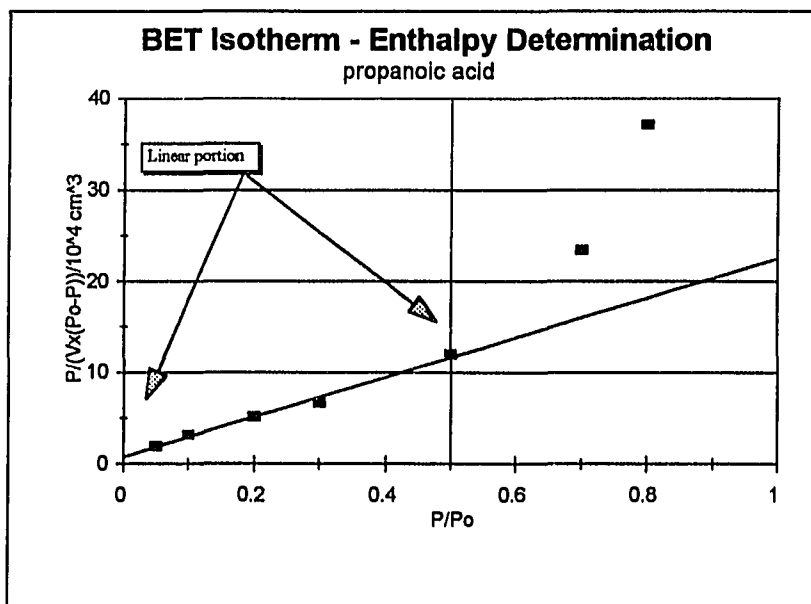


**Figure 18.** Linearized form of BET isotherm for propanoic acid interaction with 2.0 KHz PEI coated 10 MHz QCM.

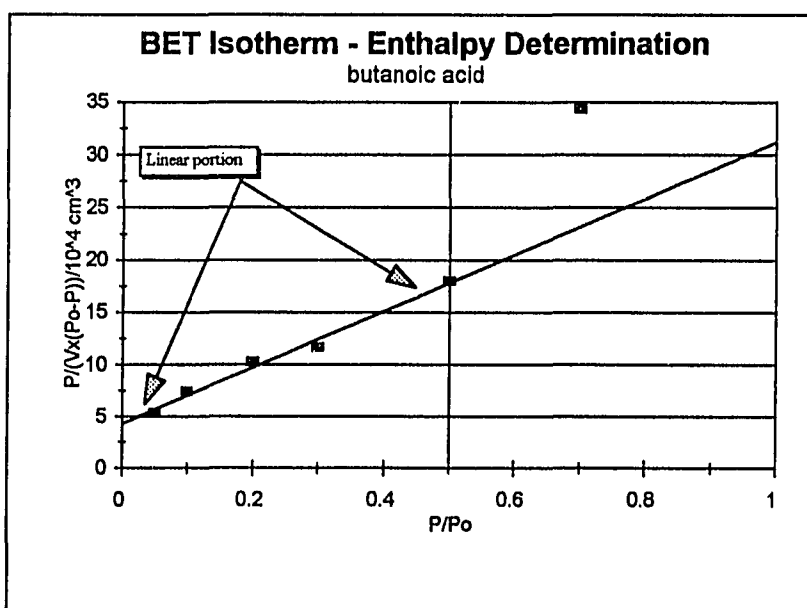


**Figure 19.** Linearized form of BET isotherm for butanoic acid interaction with 2.0 KHz PEI coated 10 MHz QCM.

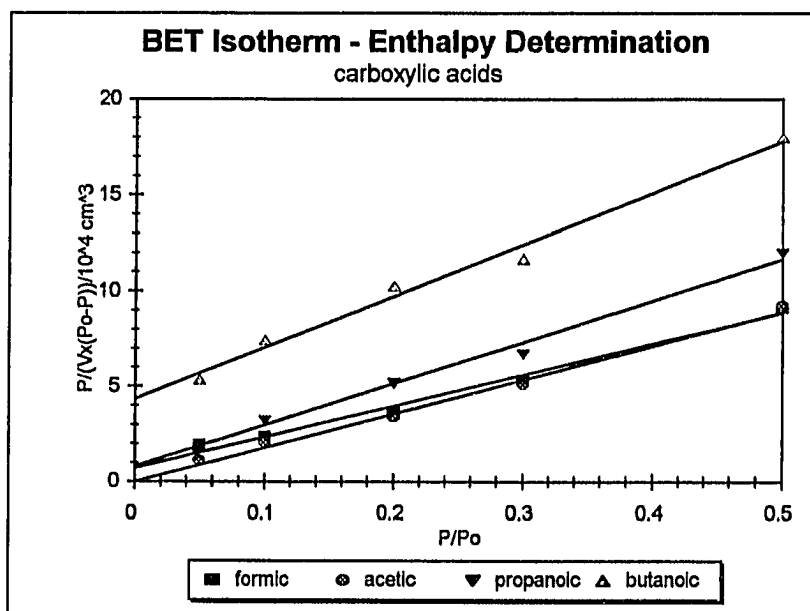


**Figure 20.** Combined linearized forms of BET isotherms for formic, acetic, propanoic, and butanoic acids interactions with 2.0 KHz PEI coated 10 MHz QCM.

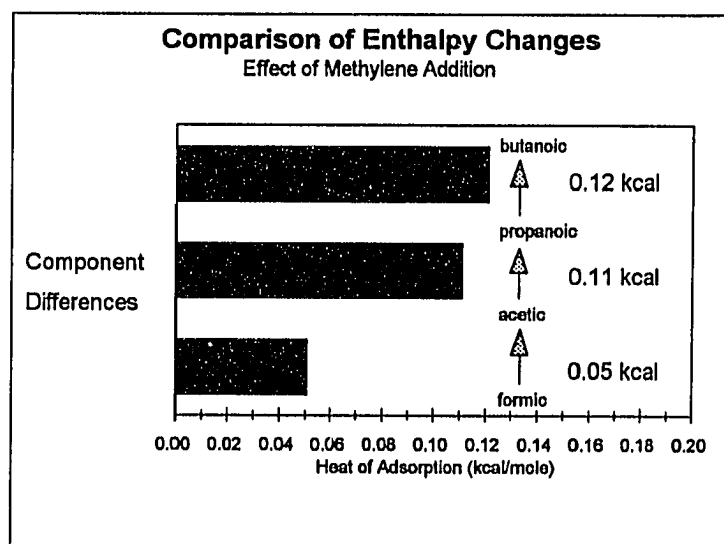


**Figure 21.** The effects of methylene addition to calculated changes in heats of adsorptions for formic, acetic, propanoic, and butanoic acids interactions with 2.0 KHz PEI coated 10 MHz QCM.

### Dilution Effects and Coating Sensitivity

Six dilutions of carboxylic acid interactions with the PEI coating were compared to determine the effects of vapor concentration on sensor sensitivity. The purpose was to ascertain whether coating responses remain constant over a series of dilutions thus enabling calculation of the LSER coating (solvent) coefficients for PEI. As mentioned in chapter 4 the partition coefficient ( $K$ ) is directly proportion to frequency change for the QCM. Frequency data for six carboxylic acids with known LSER solute values (See Table 2.) was necessary to solve for the coating coefficients using six equations (e.g. six variables -  $c$ ,  $s$ ,  $r$ ,  $a$ ,  $b$ ,  $l$ , and six equations). The six equations were solved simultaneously using Mathcad® software for six dilutions which produced six sets of LSER coating coefficients. The calculated coefficient values are summarized in Table 3.

Examination of the calculated results reveals that the value of the LSER coefficient for a parameter ( $c$ ,  $s$ ,  $r$ ,  $a$ ,  $b$ , or  $l$ ) varies with each dilution. For instance, the value of the LSER  $c$  coefficient is not the same for each of the dilutions. A plot of the  $c$  coefficient values versus the dilution is shown in Figure 22. Similiar plots were obtained for the  $s$ ,  $r$ ,  $a$ ,  $b$ , and  $l$  coefficients. (See Appendix I.)

An explanation for the different coefficient values is that at high concentrations the PEI coated sensor behaves differently because multilayering interactions between analytes increase which changes the coefficient value. At lower concentrations, monolayer adsorption begins to predominate and the value of the coating coefficient moves toward a constant value. The results suggest that care should be taken when assigning and interpreting LSER coating coefficients for a coating. At

very dilute concentrations the coefficient value differences are probably negligible.

**Table 3.**

Calculated LSER coating coefficients for PEI using frequency values obtained from the interaction of formic, acetic, propanoic, butanoic, pentanoic, and hexanoic acids.

Dilution	c	d	s	a	b	l
20x	30.302	0.412	-45.722	-0.611	-0.306	-0.811
5x	30.973	0.579	-44.603	-0.851	-0.402	-1.125
2x	31.548	0.639	-43.646	-0.948	-0.475	-1.258
1.43x	32.402	0.878	-42.221	-1.295	-0.624	-1.714
1.25x	33.024	1.085	-41.185	-1.610	-0.806	-2.173
1x	34.596	1.544	-38.565	-2.299	-1.176	-3.056

Note: The low vapor pressure of hexanoic acid at room temperature requires that frequency values be estimated at the 20x dilution from a linear regression plot of frequency values obtained at higher concentrations.

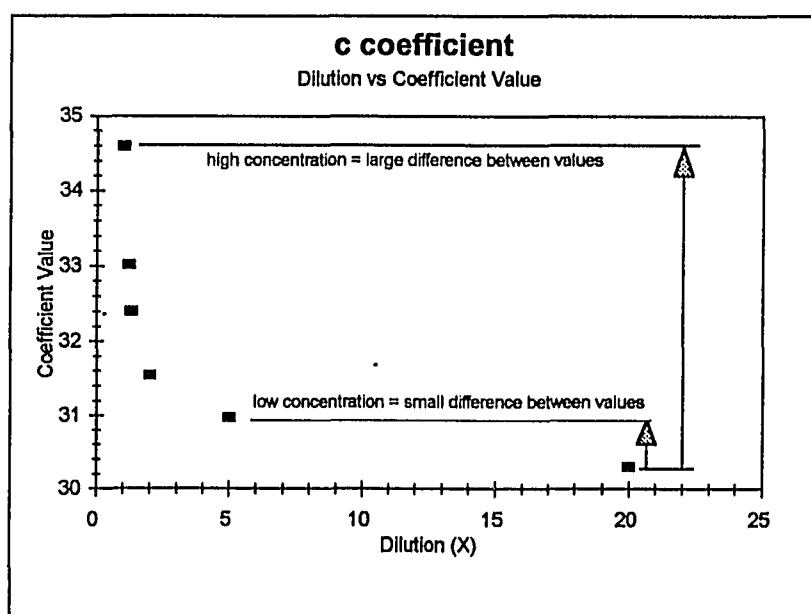


**Figure 22.** Plot indicating the variance of PEI coating coefficient values at six dilutions for formic, acetic, propanoic, butanoic, pentanoic, and hexanoic acids, a homologous series.

### Molecular Orientation Study

A series of calculations were performed to determine the molecular orientation of the analytes with the PEI coating. Semiempirical methods were used to calculate the molecular dimensions of formic, acetic, propanoic, and butanoic acids. For example, butanoic acid, a linear molecule, would fit in a rectangular box with dimensions  $2.65\text{\AA} \times 1.81\text{\AA} \times 7.81\text{\AA}$ . The surface area of the PEI coated sensor is  $1\text{ cm}^2$ . It is possible to calculate the number of molecules that could come in contact with the coating depending on the orientation of the analyte molecule. For instance, if the  $7.81\text{\AA}$  length of butanoic acid is oriented perpendicular to the surface, the  $2.65 \times 1.81\text{ \AA}^2$  side lies parallel to the surface. Dividing the total surface area by area of this side indicates  $2.08 \times 10^{15}$  molecules may attach provided that number of binding sites are available. Three orientations were considered.

The number of molecules which actually attached to the coating was calculated using the mass to frequency change relationship for the QCM. The actual number versus the calculated number of molecules varied by two to three orders of magnitude for all of the analytes. The actual number (which was experimentally determined) was always the lower number. The values ranged from  $1.48 \times 10^{11}$  to  $1.05 \times 10^{13}$  molecules.

Several semiempirical calculations were performed to determine the possible number binding sites (nitrogens) available over the  $1\text{ cm}^2$  surface area. If linear monomeric, dimeric, and trimeric forms of PEI occupy the surface, the number of binding sites available range from  $1.16\text{--}1.24 \times 10^{15}$ . This number is in accord with the calculated number of analytes available to interact. The number of binding sites decreases significantly



as polymer branching increases. For instance, the calculations indicate that a branched trimer would have  $6.82 \times 10^{13}$  binding sites, a randomly branched polymer with seven nitrogens would have approximately  $5.80 \times 10^{13}$  binding sites, and a randomly branched polymer with fifteen nitrogens would have approximately  $6.07 \times 10^{11}$  binding sites. The actual number of molecules which occupy the surface falls between the later two numbers and may indicate that significant branching of the polymer has occurred.

There is also the possibility that the coating did not occupy the entire surface area. This is not surprising. When polymer is drop coated, the coating will shrink toward the center of the drop as the solvent evaporates. The shrinking does not effect the efficiency of the QCM device.

Without a uniform layer of coating, however, it is difficult to discern the orientation of the analyte molecules to the coating. This is perhaps why numerous researchers have resorted to spectroscopic techniques, such as Raman, UV, and IR, to study orientations. Success of the study performed above would require highly accurate methods of sensor coating (e.g. Langmuir-Blodgett monolayering methods) which are expensive and time consuming.

## Chapter 5

### SUMMARY AND CONCLUSIONS

A series of experimental studies was performed. The results were compared with values obtained from computerized molecular modeling methods supplemented with chemometric methods. The purpose was to interpret, analyze, and predict sensitivity, selectivity, and other properties of solid/vapor sorption interactions with chemical recognition coatings on QCM devices.

One study was conducted to determine whether varying thicknesses of poly(ethylenimine) (PEI) coating on a QCM would produce a linear response when exposed to the individual vapors of a homologous series of carboxylic acid vapors and to determine the relative sensitivity of the PEI coating for each of the vapors. The results indicate that all of the acid analytes produce highly linear responses with regard to coating thickness and sensitivity. The results further suggest that analyses of the slopes reveal increased selectivity of the PEI coating toward analytes of increasing aliphatic chain length due mainly to dispersive interactions. Decreasing polarizability interactions may contribute; however, since PEI is basically a non-polarizing coating, these interactions were considered to be minimal. A linear relationship between calculated van der Waals force

values obtained from semiempirical molecular modeling software and the log of the slopes of the experimentally obtained dispersion force values may exist. The ratio of the slopes coincided with the ratio of the calculated vdW force values. Calculated dipole moments and dispersion force values appear to coincide trendwise with experimentally determined LSER values (Appendix I). One concern which has not been investigated in this research is that a fundamental problem may arise with regard to interpreting the selectivity of unknown concentrations of acid analytes. Currently, a major limitation to a complete theoretical model is that molecular modeling does not provide acidic and basic hydrogen-bonding values which can be related to experimentally determined LSER values.

Isotherm studies were conducted to determine the energy of absorption between the solid phase and the analytes and to discern whether physical adsorption or chemisorption processes occur. The solid/vapor interactions exhibit reversibility which may describe physical adsorption processes. Linearized BET isotherm plots tend to validate this notion by indicating that the values for the heats of adsorption for the interactions numerically fall within the range of physical adsorption processes.

The effects of vapor concentration on sensor coating sensitivity indicate that coating responses change significantly relative to analyte concentration. Calculation of the LSER coating (solvent) coefficients for PEI indicate that at high concentrations the PEI coated sensor may behave differently because multilayering interactions between analytes increase which change the coefficient values. At lower concentrations, monolayer adsorption may predominate and the values of the coating coefficients move toward more constant values. Coefficient value differences become

negligible at very dilute concentrations; however, at higher concentrations care should be taken when assigning and interpreting LSER coating coefficients for a particular coating. Calculations indicate that incomplete coverage of the QCM surface area impede the determination of the molecular orientation of the analyte molecules with respect to the coating. The experimentally obtained number of molecules capable of binding is much lower than calculated numbers of molecules for three orientations.

In summary, molecular modeling software may be useful for determining trendwise the relative sensitivity and selectivity of a particular coating towards a set of analytes by providing parameters such as dipolarity, polarizability, and dispersion force values in a similar manner to those values obtained from LSER tables. However, current modeling software packages lack built-in capabilities to quantitatively evaluate acidic and basic hydrogen-bonding characteristics. These capabilities are probably necessary to formulate a complete theoretical model based entirely on computerized molecular modeling technology. It is further suggested that supplementary experimental procedures such as isotherm studies and vapor concentrations studies be performed to help elucidate the processes of analyte vapor interactions with chemical recognition coatings on QCM sensors.

The present research relates to the potential utility of computerized molecular modeling and chemometric methods in predicting interactions which can be used as a basis for selecting recognition coatings. The problem is obviously a major one which has been addressed for many years by numerous investigators. Results from the thesis research will hopefully contribute to the existing information base and form the basis of additional investigations.

## Chapter 6

### **FUTURE WORK**

The research performed here raises numerous questions which are not easily answered. Molecular modeling methods that can quantitatively evaluate acidic and basic hydrogen-bonding characteristics might aid in developing a model which accurately depicts vapor interactions with recognition coatings. Although molecular modeling and chemometric analysis can provide information regarding the sensitivity and selectivity of solid/vapor interactions, it also suggests that any one particular coating may not be capable of discriminating between a mixture of analytes due to varying concentrations. It is the general consensus of researchers in the field of mass sensor technology that the utilization of sensor arrays (groups of sensors) composed of a variety of recognition coatings may provide improved selectivity. This method incorporates the use of pattern recognition techniques and modern neural network technologies. Using a sensor array, each analyte will exhibit a unique "fingerprint" which is discernible by pattern recognition. The neural network is capable of statistically evaluating the presence of the analyte with respect to other interferences. A tremendous amount of work in this field is foreseen. A major area of future work with mass sensors is anticipated to be

development of software for predicting analyte/coating interactions;  
another is frequency wave shape study and interpretation.

## **APPENDIX I**

### **RAW DATA AND CALCULATIONS**

## FILM THICKNESS AND SENSITIVITY

Frequency Change versus Coating Thickness

	Coating Thickness					
	0.69	0.76	1.7	4.1	4.4	r <sup>2</sup>
<b>Frequency</b>						
formic	64	60	137	448		0.989
acetic	93	146	266	798	807	0.990
propanoic	180	228	577	1966		0.995
butanoic	540	829	2236	7624	7861	0.993
pentanoic	1192	1228	4935	15555	15853	0.995
<b>LSER Values</b>						
	polarizability	dipolarity	acid H-bonding	basic H-bonding	dispersion	
acetic	0.265	0.60	0.55	0.43	1.750	
propanoic	0.233	0.60	0.54	0.43	2.290	
butanoic	0.210	0.60	0.54	0.42	2.830	
pentanoic	0.205	0.60	0.54	0.41	3.380	
hexanoic	0.174	0.60	0.54	0.39	3.920	
heptanoic	0.149	0.60	0.54	0.38	4.460	



# ISOTHERM STUDY

VP is vapor pressure in mm Hg at 20 C

MW is molecular weight

NA means the value is not available

FORMIC VP=35 MW=46.03	average frequency change (Hz)	percent flow nitrogen	percent flow acid	dilution	concentration mg/cubic M	concentration/100 mg/cubic M	corrected frequency Hz/mg/cubic M x100
	818	95	5	20.00	4.41E+03	44	19
	1300	90	10	10.00	8.82E+03	88	15
	1905	80	20	5.00	1.76E+04	176	11
	2241	70	30	3.33	2.65E+04	265	8
	3088	50	50	2.00	4.41E+04	441	7
	4095	30	70	1.43	6.18E+04	618	7
	4456	20	80	1.25	7.06E+04	706	6
	7993	0	100	1.00	8.82E+04	882	9

ACETIC VP=11.04 MW=60.06	average frequency change (Hz)	percent flow nitrogen	percent flow acid	dilution	concentration mg/cubic M	concentration/100 mg/cubic M	corrected frequency Hz/mg/cubic M x100
	1107	95	5	20.00	1.87E+03	19	59
	1302	90	10	10.00	3.75E+03	37	35
	1773	80	20	5.00	7.50E+03	75	24
	2025	70	30	3.33	1.12E+04	112	18
	2605	50	50	2.00	1.87E+04	187	14
	3378	30	70	1.43	2.62E+04	262	13
	3628	20	80	1.25	3.00E+04	300	12
	5136	0	100	1.00	3.75E+04	375	14

<b>PROPANOIC</b> <b>VP=2.9</b> <b>MW=74.08</b>	<b>average</b>	<b>percent</b>	<b>percent</b>				<b>corrected</b>
	<b>frequency</b>	<b>flow</b>	<b>flow</b>		<b>concentration</b>	<b>concentration/100</b>	<b>frequency</b>
	<b>change (Hz)</b>	<b>nitrogen</b>	<b>acid</b>	<b>dilution</b>	<b>mg/cubic M</b>	<b>mg/cubic M</b>	<b>Hz/mg/cubic M x100</b>
	611	95	5	20.00	5.88E+02	6	104
	791	90	10	10.00	1.18E+03	12	67
	1102	80	20	5.00	2.35E+03	24	47
	1459	70	30	3.33	3.53E+03	35	41
	1905	50	50	2.00	5.88E+03	59	32
	2270	30	70	1.43	8.24E+03	82	28
	2456	20	80	1.25	9.41E+03	94	26
	2966	0	100	1.00	1.18E+04	118	25

<b>BUTANOIC</b> <b>VP=0.43</b> <b>MW=88.11</b>	<b>average</b>	<b>percent</b>	<b>percent</b>				<b>corrected</b>
	<b>frequency</b>	<b>flow</b>	<b>flow</b>		<b>concentration</b>	<b>concentration/100</b>	<b>frequency</b>
	<b>change (Hz)</b>	<b>nitrogen</b>	<b>acid</b>	<b>dilution</b>	<b>mg/cubic M</b>	<b>mg/cubic M</b>	<b>Hz/mg/cubic M x100</b>
	217	95	5	20.00	1.04E+02	1	209
	330	90	10	10.00	2.07E+02	2	159
	538	80	20	5.00	4.15E+02	4	130
	809	70	30	3.33	6.22E+02	6	130
	1225	50	50	2.00	1.04E+03	10	118
	1497	30	70	1.43	1.45E+03	15	103
	NA	20	80	1.25	1.66E+03	17	NA
	1785	0	100	1.00	2.07E+03	21	86

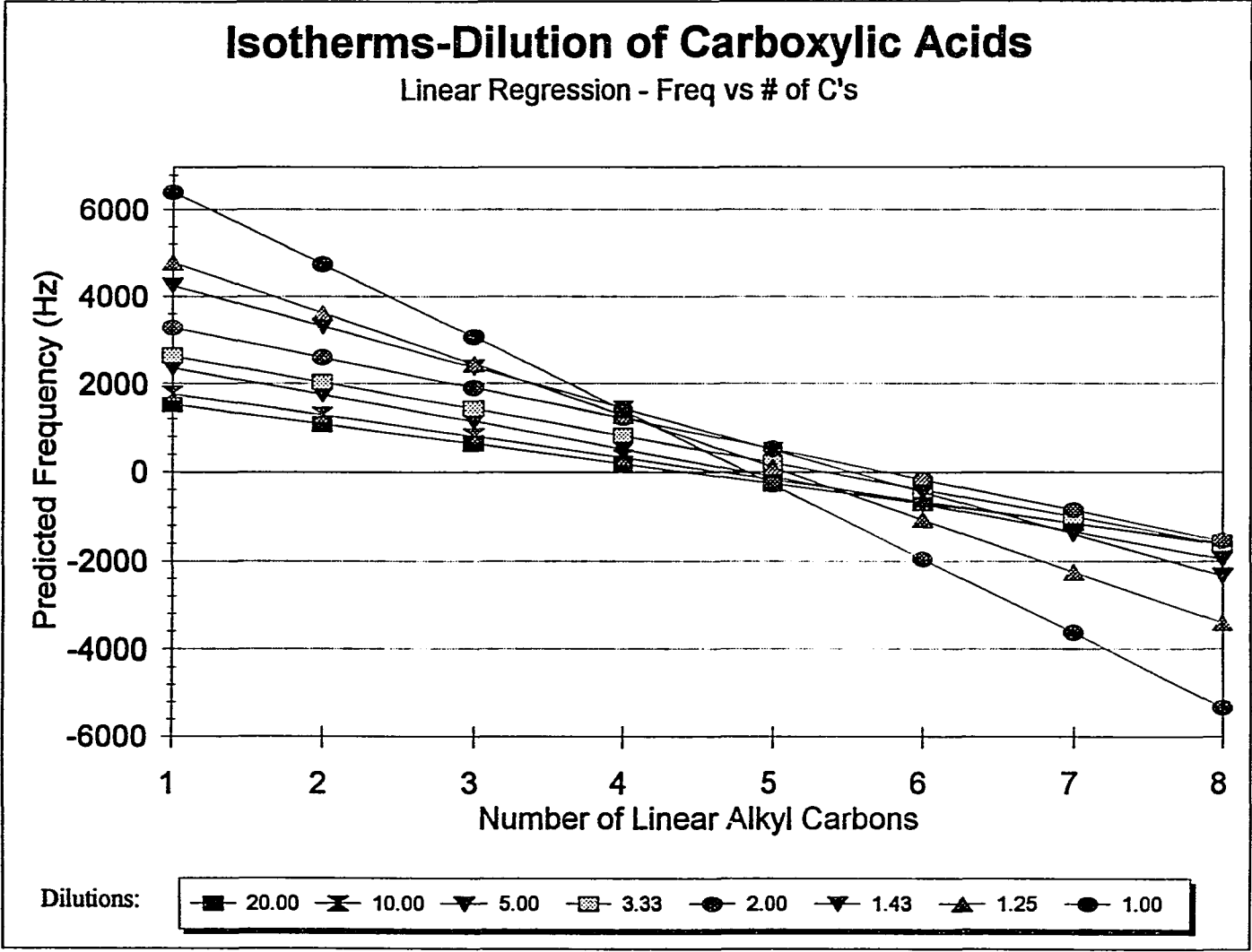
Concentration Calculation:

((vapor pressure/(760 mm Hg x 0.082 x 293)) x molecular weight x 1000 x1000)/dilution

Corrected Frequency Calculation:

(frequency change/concentration)

<b>Enthalpy Determination</b>					
<i>formic</i>					
1.81	0.05	Regression Output:		<b>ENTHALPY</b>	<b>ENTHALPY</b>
2.4	0.1	Constant	0.728906	L atm/	kcal/
3.68	0.2	Std Err of Y Est	0.302197	K mol	K mol
5.37	0.3	R Squared	0.991975	67.01	1.6238
9.09	0.5	No. of Observations	5		
		Degrees of Freedom	3		
		X Coefficient(s)	16.26563		
		Std Err of Coef.	0.844666		
<i>acetic</i>					
1.15	0.05	Regression Output:		<b>ENTHALPY</b>	<b>ENTHALPY</b>
2.06	0.1	Constant	0.097148	L atm/	kcal/
3.4	0.2	Std Err of Y Est	0.317292	K mol	K mol
5.11	0.3	R Squared	0.992625	69.20	1.6769
9.26	0.5	No. of Observations	5		
		Degrees of Freedom	3		
		X Coefficient(s)	17.82109		
		Std Err of Coef.	0.886859		
<i>propanoic</i>					
1.97	0.05	Regression Output:		<b>ENTHALPY</b>	<b>ENTHALPY</b>
3.2	0.1	Constant	0.815	L atm/	kcal/
5.18	0.2	Std Err of Y Est	0.424892	K mol	K mol
6.7	0.3	R Squared	0.991094	73.94	1.7916
11.98	0.5	No. of Observations	5		
		Degrees of Freedom	3		
		X Coefficient(s)	21.7		
		Std Err of Coef.	1.18761		
<i>butanoic</i>					
5.35	0.05	Regression Output:		<b>ENTHALPY</b>	<b>ENTHALPY</b>
7.43	0.1	Constant	4.355742	L atm/	kcal/
10.25	0.2	Std Err of Y Est	0.614539	K mol	K mol
11.68	0.3	R Squared	0.98792	79.10	1.9168
18.01	0.5	No. of Observations	5		
		Degrees of Freedom	3		
		X Coefficient(s)	26.90547		
		Std Err of Coef.	1.71769		



## Example of the Solution of Six Simultaneous Equations using Mathcad

Frequency Change Values were Calculated from Linear Regression Plots of Experimental Data

Poly(ethylenimine) coating with 1.25X dilutions of acetic, propanoic, butanoic, pentanoic, hexanoic, and heptanoic acids.

	Frequency (Hz)	
acetic	3628	
propanoic	2456	Guess values=
butanoic	1284	c := 0
pentanoic	112	d := 0
hexanoic	- 1060	s := 0
heptanoic	- 2232	a := 0
		b := 0
		l := 0

Given

$$\begin{aligned}
 c + (0.265 \cdot d) + (0.60 \cdot s) + (0.55 \cdot a) + (0.43 \cdot b) + (1.750 \cdot l) &= 3.628 \\
 c + (0.233 \cdot d) + (0.60 \cdot s) + (0.54 \cdot a) + (0.43 \cdot b) + (2.290 \cdot l) &= 2.456 \\
 c + (0.210 \cdot d) + (0.60 \cdot s) + (0.54 \cdot a) + (0.42 \cdot b) + (2.830 \cdot l) &= 1.284 \\
 c + (0.205 \cdot d) + (0.60 \cdot s) + (0.54 \cdot a) + (0.41 \cdot b) + (3.380 \cdot l) &= 1.112 \\
 c + (0.174 \cdot d) + (0.60 \cdot s) + (0.54 \cdot a) + (0.39 \cdot b) + (3.920 \cdot l) &= -1.060 \\
 c + (0.149 \cdot d) + (0.60 \cdot s) + (0.54 \cdot a) + (0.38 \cdot b) + (4.460 \cdot l) &= -2.232
 \end{aligned}$$

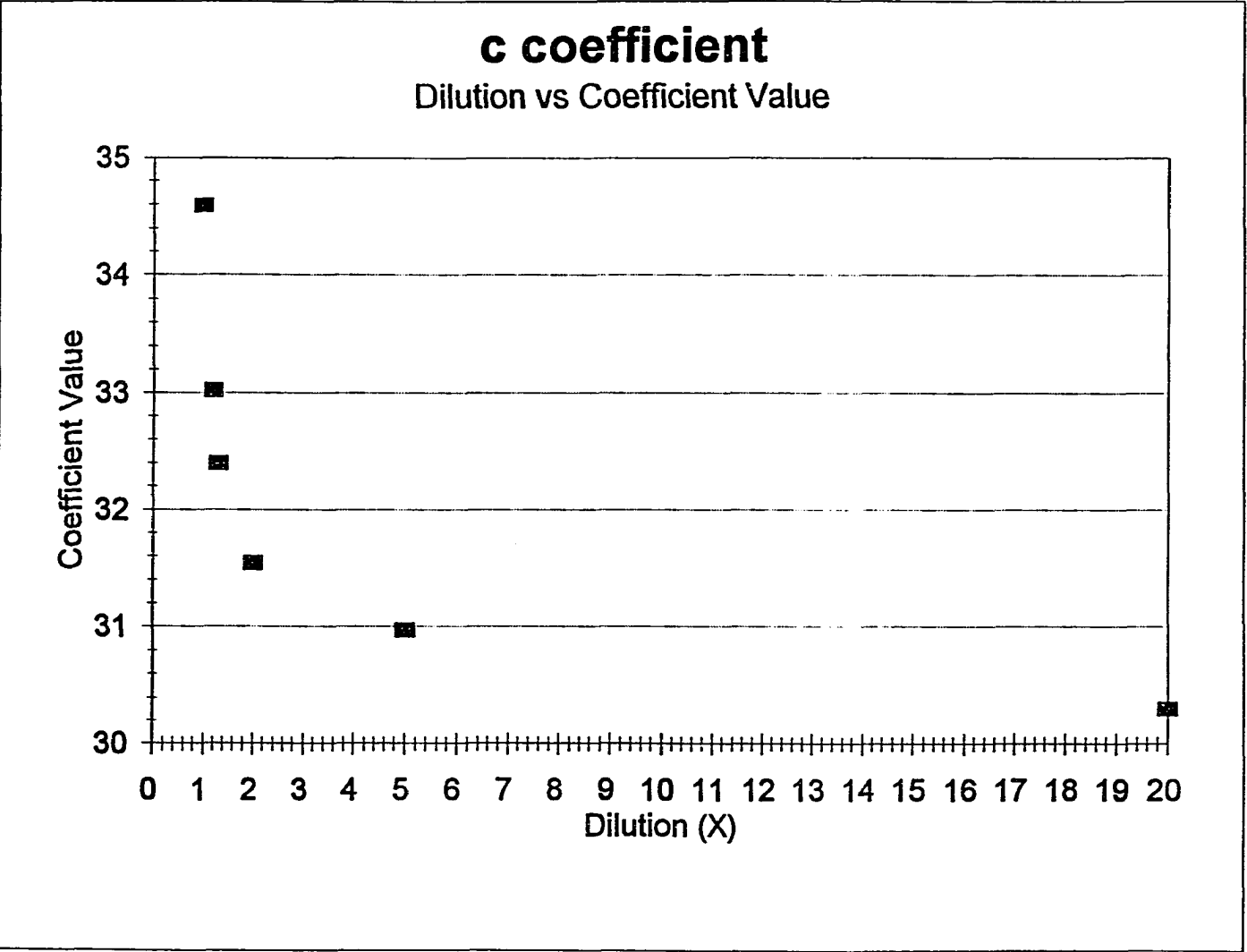
$$\begin{bmatrix} \text{cval} \\ \text{dval} \\ \text{sval} \\ \text{aval} \\ \text{bval} \\ \text{lval} \end{bmatrix} := \text{Find}(c, d, s, a, b, l)$$

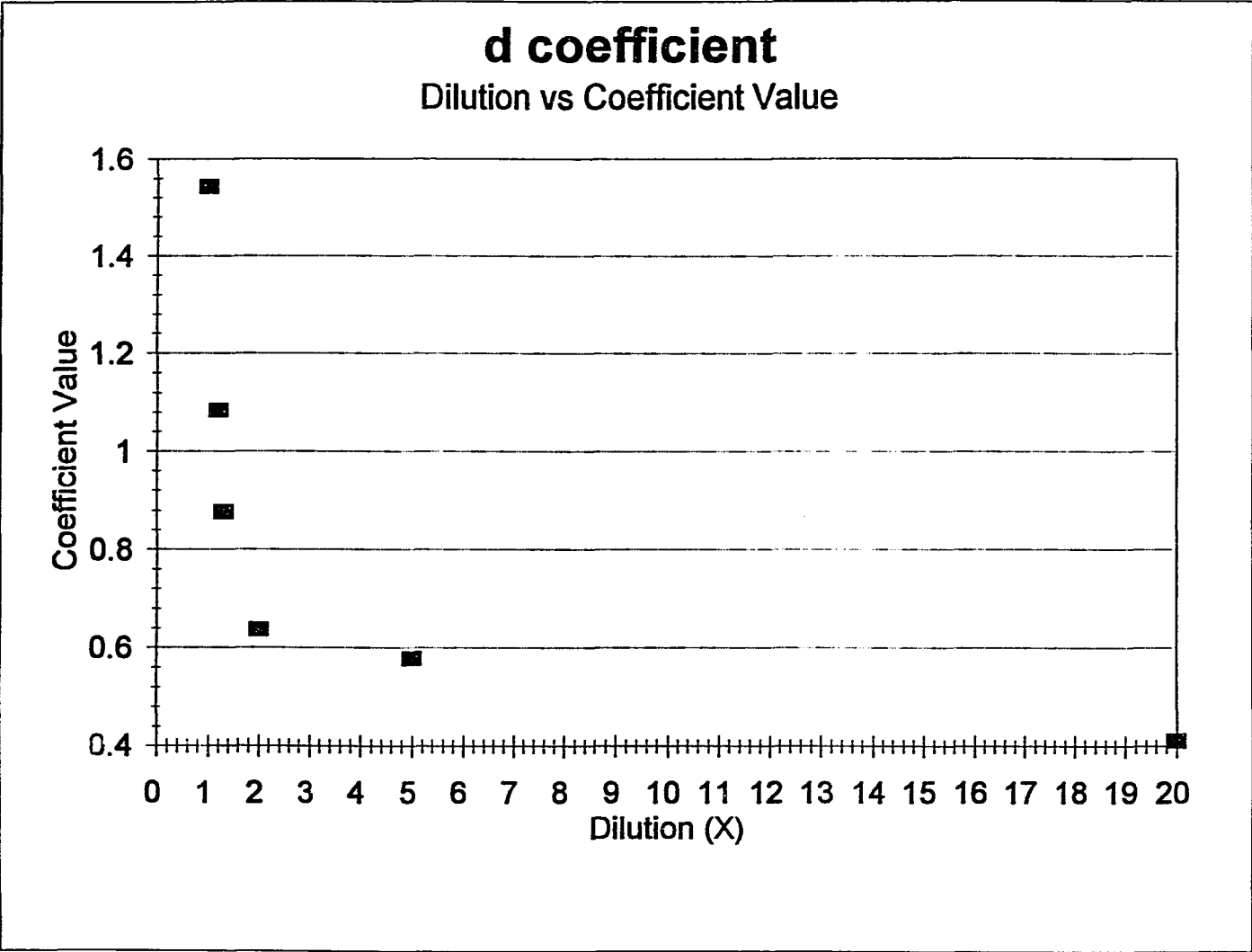
$$\begin{aligned}
 \text{cval} &= 33.024 \\
 \text{dval} &= 1.085 \\
 \text{sval} &= -41.185 \\
 \text{aval} &= -1.61 \\
 \text{bval} &= -0.806 \\
 \text{lval} &= -2.137
 \end{aligned}$$

### **Poly(ethylenimine) Coating Coefficients at Various Dilutions**

Calculated from linear regression frequency values for a carboxylic acid series

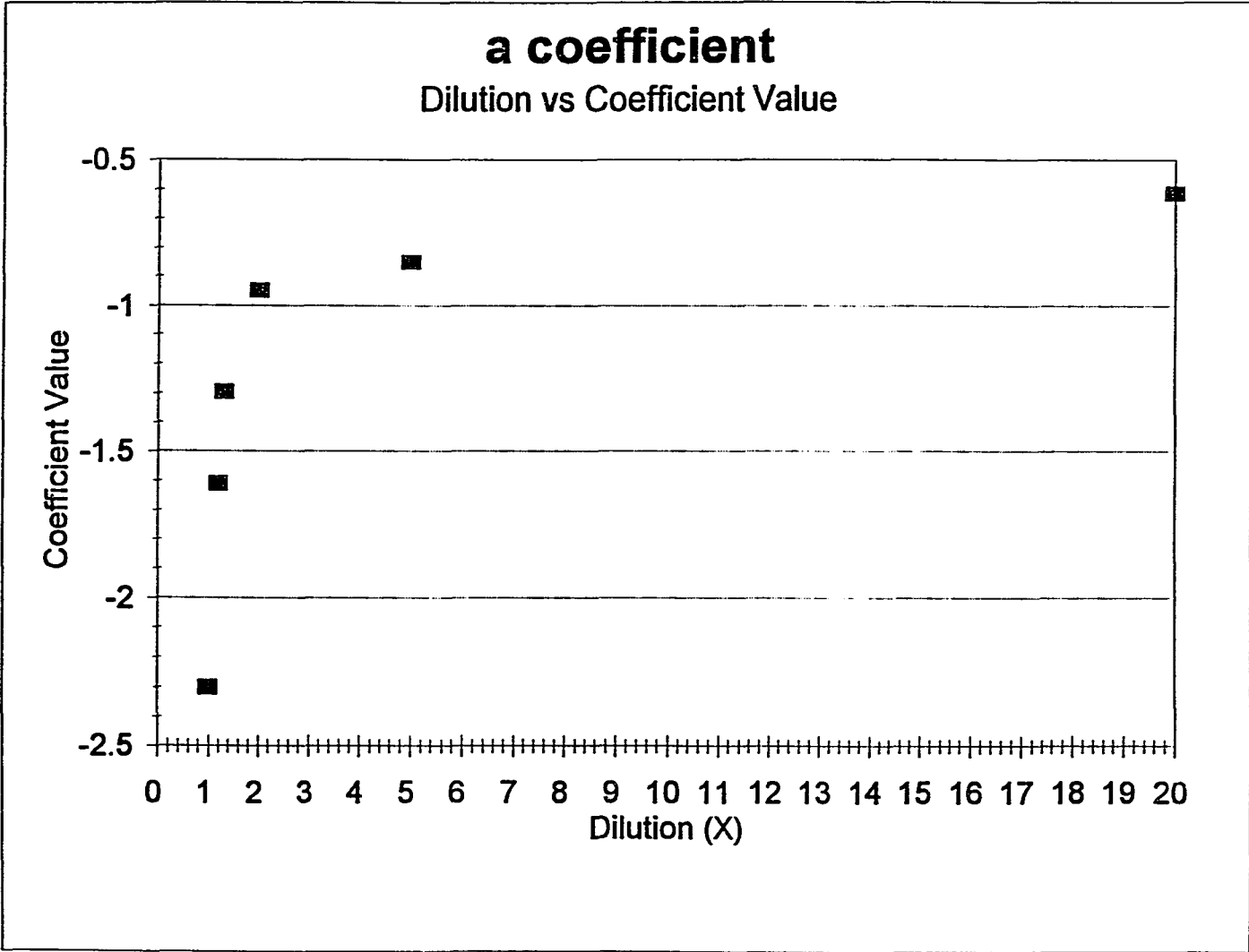
	<b>20x</b>	<b>5x</b>	<b>2x</b>	<b>1.43x</b>	<b>1.25x</b>	<b>1x</b>
<b>c</b>	30.302	30.973	31.548	32.402	33.024	34.596
<b>d</b>	0.412	0.579	0.639	0.878	1.085	1.544
<b>s</b>	-45.722	-44.603	-43.646	-42.221	-41.185	-38.565
<b>a</b>	-0.611	-0.851	-0.948	-1.295	-1.610	-2.299
<b>b</b>	-0.306	-0.402	-0.475	-0.624	-0.806	-1.176
<b>l</b>	-0.811	-1.125	-1.258	-1.714	-2.173	-3.056

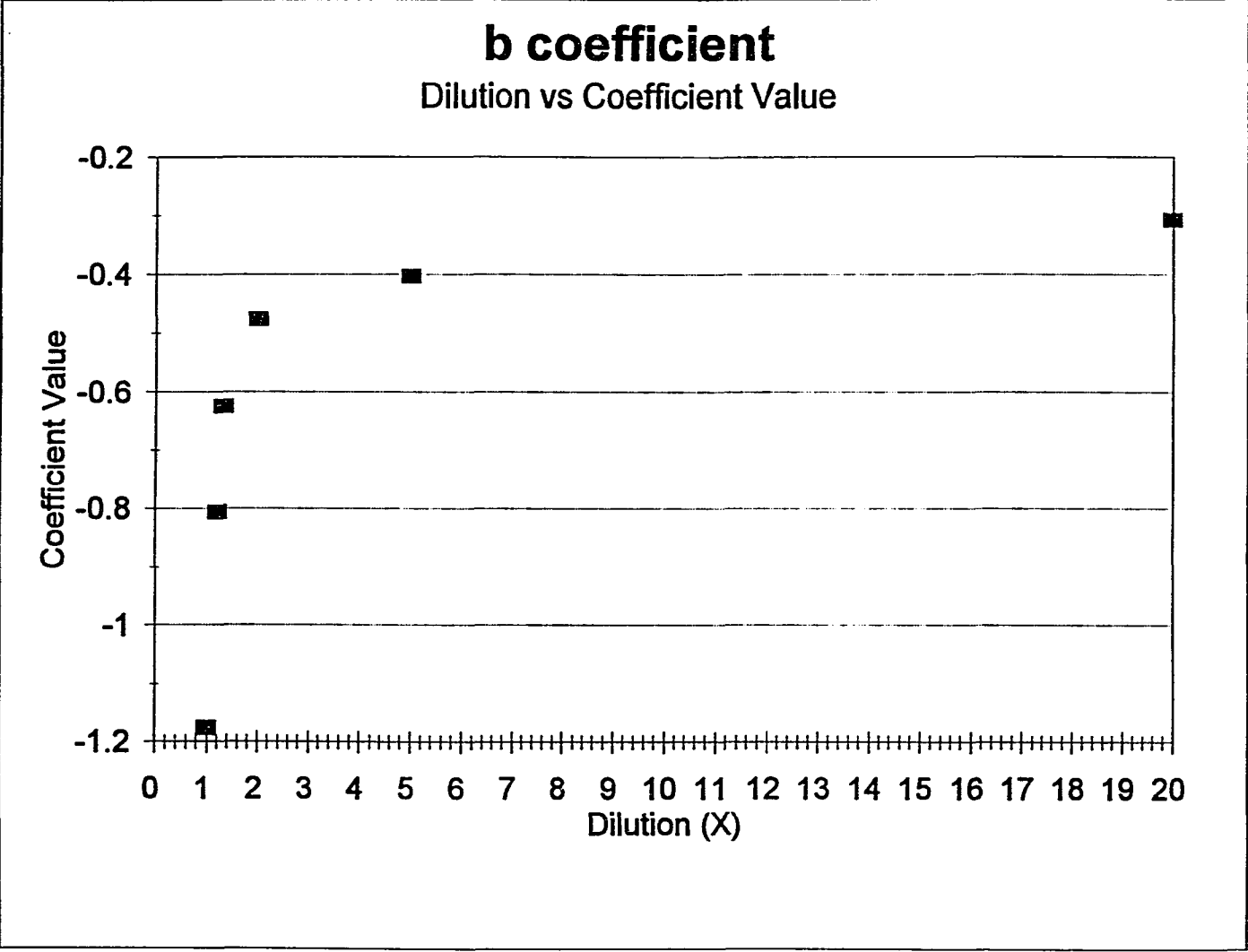


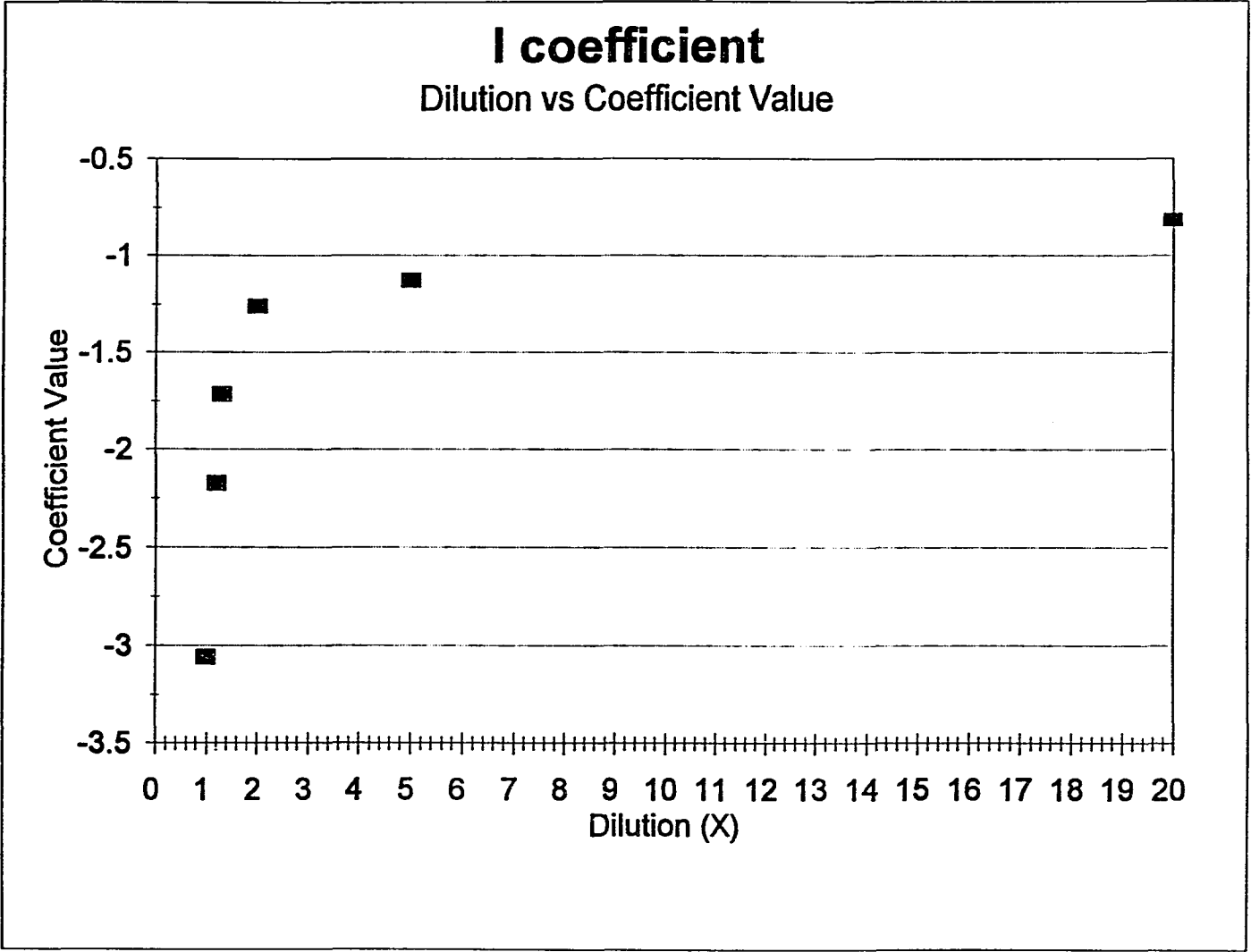












## MOLECULAR ORIENTATION STUDY

	experimental		actual	number of	number of	number of
	frequency (Hz)	dilution	number of molecules	number of molecules	molecules	molecules
				small	medium	large
formic	818	20x	1.07E+12	7.12E+15	6.85E+15	1.89E+15
	1300	10x	1.70E+12	7.12E+15	6.85E+15	1.89E+15
	1905	5x	2.49E+12	7.12E+15	6.85E+15	1.89E+15
	2241	3.33x	2.93E+12	7.12E+15	6.85E+15	1.89E+15
	3088	2.00x	4.04E+12	7.12E+15	6.85E+15	1.89E+15
	4095	1.43x	5.36E+12	7.12E+15	6.85E+15	1.89E+15
	4456	1.25x	5.83E+12	7.12E+15	6.85E+15	1.89E+15
	7993	1.00x	1.05E+13	7.12E+15	6.85E+15	1.89E+15

	experimental		actual	number of	number of	number of
	frequency (Hz)	dilution	number of molecules	number of molecules	molecules	molecules
				small	medium	large
acetic	1107	20x	1.11E+12	2.49E+15	1.55E+15	1.27E+15
	1302	10x	1.31E+12	2.49E+15	1.55E+15	1.27E+15
	1773	5x	1.78E+12	2.49E+15	1.55E+15	1.27E+15
	2025	3.33x	2.03E+12	2.49E+15	1.55E+15	1.27E+15
	2605	2.00x	2.61E+12	2.49E+15	1.55E+15	1.27E+15
	3378	1.43x	3.39E+12	2.49E+15	1.55E+15	1.27E+15
	3628	1.25x	3.64E+12	2.49E+15	1.55E+15	1.27E+15
	5136	1.00x	5.15E+12	2.49E+15	1.55E+15	1.27E+15

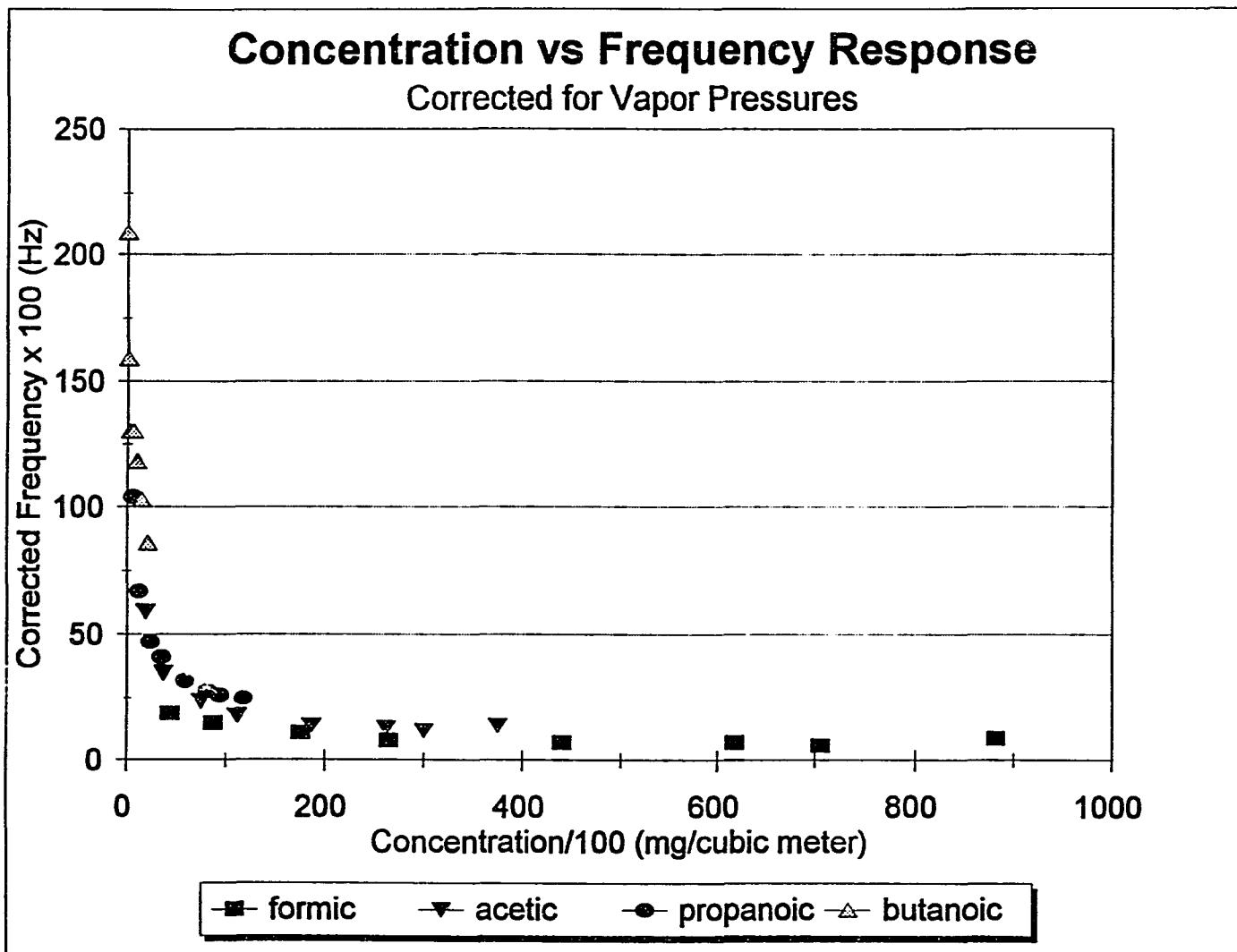
	experimental		actual	number of	number of	number of
	frequency (Hz)	dilution	number of molecules	number of molecules	molecules	molecules
				small	medium	large
propanoic	611	20x	4.97E+11	2.04E+15	1.04E+15	6.95E+14
	791	10x	6.43E+11	2.04E+15	1.04E+15	6.95E+14
	1102	5x	8.96E+11	2.04E+15	1.04E+15	6.95E+14
	1459	3.33x	1.19E+12	2.04E+15	1.04E+15	6.95E+14
	1905	2.00x	1.55E+12	2.04E+15	1.04E+15	6.95E+14
	2270	1.43x	1.84E+12	2.04E+15	1.04E+15	6.95E+14
	2456	1.25x	2.00E+12	2.04E+15	1.04E+15	6.95E+14
	2966	1.00x	2.41E+12	2.04E+15	1.04E+15	6.95E+14

	experimental		actual	number of	number of	number of
	frequency (Hz)	dilution	number of molecules	number of molecules	molecules	molecules
				small	medium	large
butanoic	217	20x	1.48E+11	2.08E+15	7.07E+14	4.83E+14
	330	10x	2.25E+11	2.08E+15	7.07E+14	4.83E+14
	538	5x	3.68E+11	2.08E+15	7.07E+14	4.83E+14
	809	3.33x	5.53E+11	2.08E+15	7.07E+14	4.83E+14
	1225	2.00x	8.37E+11	2.08E+15	7.07E+14	4.83E+14
	1497	1.43x	1.02E+12	2.08E+15	7.07E+14	4.83E+14
	na	1.25x	na	2.08E+15	7.07E+14	4.83E+14
	1785	1.00x	1.22E+12	2.08E+15	7.07E+14	4.83E+14

na means value not available

## APPENDIX II

### **ADDITIONAL DATA TABLES AND FIGURES**



## Polyethylenimine Interactions

- 1 methanol
- 2 acetic acid
- 3 n-pentane
- 4 cyclohexane
- 5 benzene
- 6 ethylbenzene
- 7 2-propanol

	c	r	s	a	b	l	
<b>123456</b>	-0.521	-0.573	1.523	5.190	-4.985	0.242	
<b>234567</b>	-0.436	-0.476	1.129	4.435	-3.568	0.203	
<b>134567</b>	-0.288	-0.307	0.449	1.510	-1.123	0.134	
<b>124567</b>	-0.062	-2.636	2.455	3.670	-4.375	0.300	
<b>123567</b>	-0.627	-1.908	2.489	3.628	-3.466	0.291	
<b>123467</b>	-0.886	-0.989	1.019	4.758	-3.312	0.411	
<b>123457</b>	-0.863	-0.963	1.379	4.419	-3.407	0.400	
<b>acetic acid</b>		<b>R</b>	<b>PI</b>	<b>AH</b>	<b>BH</b>	<b>LogL16</b>	
		0.265	0.6	0.55	0.43	1.75	
	c	rR	sPI	aAH	bBH	lLogL16	Log K'
<b>123456</b>	-0.521	-0.152	0.914	2.855	-2.144	0.424	1.375
<b>234567</b>	-0.436	-0.126	0.677	2.439	-1.534	0.355	1.376
<b>124567</b>	-0.062	-0.699	1.473	2.019	-1.881	0.525	1.375
<b>123567</b>	-0.627	-0.508	1.493	1.995	-1.490	0.509	1.375
<b>123467</b>	-0.886	-0.262	0.611	2.617	-1.424	0.719	1.375
<b>123457</b>	-0.863	-0.255	0.827	2.430	-1.465	0.700	1.375
<b>average</b>	-0.566	-0.333	0.999	2.393	-1.656	0.539	1.375
<b>std dev</b>	0.308	0.224	0.390	0.336	0.290	0.148	0.000
<b>high</b>	-0.260	-0.110	1.389	2.729	-1.366	0.685	1.375
<b>low</b>	-0.872	-0.557	0.610	2.056	-1.947	0.393	1.375
<b>134567</b>	-0.288	-0.081	0.269	0.831	-0.483	0.235	0.482
	c	r	s	a	b	l	
<b>123456</b>	-0.521	-0.573	1.523	5.190	-4.985	0.242	
<b>234567</b>	-0.436	-0.476	1.129	4.435	-3.568	0.203	
<b>134567</b>	-0.288	-0.307	0.449	1.510	-1.123	0.134	
<b>124567</b>	-0.062	-2.636	2.455	3.670	-4.375	0.300	
<b>123567</b>	-0.627	-1.908	2.489	3.628	-3.466	0.291	
<b>123467</b>	-0.886	-0.989	1.019	4.758	-3.312	0.411	
<b>123457</b>	-0.863	-0.963	1.379	4.419	-3.407	0.400	
<b>methanol</b>		<b>R</b>	<b>PI</b>	<b>AH</b>	<b>BH</b>	<b>LogL16</b>	
		0.278	0.4	0.37	0.41	0.922	
	c	rR	sPI	aAH	bBH	lLogL16	Log K'
<b>123456</b>	-0.521	-0.159	0.609	1.920	-2.044	0.223	0.028
<b>134567</b>	-0.288	-0.085	0.180	0.559	-0.460	0.124	0.028
<b>124567</b>	-0.062	-0.733	0.982	1.358	-1.794	0.277	0.028
<b>123567</b>	-0.627	-0.530	0.996	1.342	-1.421	0.268	0.028
<b>123467</b>	-0.886	-0.275	0.408	1.760	-1.358	0.379	0.028
<b>123457</b>	-0.863	-0.268	0.552	1.635	-1.397	0.369	0.028
<b>average</b>	-0.541	-0.342	0.621	1.429	-1.412	0.273	0.028
<b>std dev</b>	0.324	0.244	0.321	0.482	0.539	0.095	0.000
<b>high</b>	-0.217	-0.098	0.942	1.912	-0.673	0.368	0.028
<b>low</b>	-0.865	-0.588	0.300	0.947	-1.952	0.178	0.028
<b>234567</b>	-0.436	-0.132	0.452	1.641	-1.463	0.187	0.249



## Relative Interaction Affinities

### Poly(ethylenimine) With Other Compounds

PEI	c	r	s	a	b	l	
	-52.15	-57.324	152.27	519.018	-498.494	24.213	
<b>ACIDS</b>		<b>R2</b>	<b>PI</b>	<b>AH</b>	<b>BH</b>	<b>logL16</b>	
acetic acid		0.265	0.60	0.55	0.43	1.750	
propanoic acid		0.233	0.60	0.54	0.43	2.290	
butanoic acid		0.210	0.60	0.54	0.42	2.830	
pentanoic acid		0.205	0.60	0.54	0.41	3.380	
hexanoic acid		0.174	0.60	0.54	0.39	3.920	
heptanoic acid		0.149	0.60	0.54	0.38	4.460	
	<b>c</b>	<b>rR2</b>	<b>sPi</b>	<b>aAH</b>	<b>bBH</b>	<b>llogL16</b>	<b>logK'</b>
acetic acid	-52.15	-15.191	91.36	285.46	-214.352	42.373	137.500
propanoic acid	-52.15	-13.356	91.36	280.27	-214.352	55.448	147.220
butanoic acid	-52.15	-12.038	91.36	280.27	-209.367	68.523	166.598
pentanoic acid	-52.15	-11.751	91.36	280.27	-204.383	81.840	185.187
hexanoic acid	-52.15	-9.974	91.36	280.27	-194.413	94.915	210.009
heptanoic acid	-52.15	-8.541	91.36	280.27	-189.428	107.990	229.502

PEI	c	r	s	a	b	l	
	-52.15	-57.324	152.27	519.018	-498.494	24.213	
<b>ALCOHOLS</b>		<b>R2</b>	<b>Pi</b>	<b>AH</b>	<b>BH</b>	<b>logL16</b>	
ethanol		0.246	0.40	0.33	0.44	1.485	
propanol		0.236	0.40	0.33	0.45	2.097	
butanol		0.224	0.40	0.33	0.45	2.601	
pentanol		0.219	0.40	0.33	0.45	3.106	
hexanol		0.210	0.40	0.33	0.45	3.610	
heptanol		0.211	0.40	0.32	0.45	4.115	
	<b>c</b>	<b>rR2</b>	<b>sPi</b>	<b>aAH</b>	<b>bBH</b>	<b>llogL16</b>	<b>logK'</b>
ethanol	-52.15	-14.102	60.91	171.28	-219.337	35.956	-17.449
propanol	-52.15	-13.528	60.91	171.28	-224.322	50.775	-7.042
butanol	-52.15	-12.841	60.91	171.28	-224.322	62.978	5.849
pentanol	-52.15	-12.554	60.91	171.28	-224.322	75.206	18.363
hexanol	-52.15	-12.044	60.91	171.28	-224.322	87.409	31.077
heptanol	-52.15	-12.095	60.91	166.09	-224.322	99.636	38.063

<b>PEI</b>	<b>-52.15</b>	<b>-57.324</b>	<b>152.27</b>	<b>519.018</b>	<b>-498.494</b>	<b>24.213</b>	
<b>ACETATE ESTERS</b>		<b>R2</b>	<b>Pi</b>	<b>AH</b>	<b>BH</b>	<b>logL16</b>	
ethyl acetate		0.106	0.55	0.00	0.45	2.376	
n-propyl acetate		0.092	0.55	0.00	0.45	2.878	
n-butyl acetate		0.071	0.55	0.00	0.45	3.379	
pentyl acetate		0.067	0.55	0.00	0.45	3.810	
	<b>c</b>	<b>rR2</b>	<b>sPi</b>	<b>aAH</b>	<b>bBH</b>	<b>llogL16</b>	<b>logK'</b>
ethyl acetate	-52.15	-6.076	83.75	0.00	-224.322	57.530	-141.271
n-propyl acetate	-52.15	-5.274	83.75	0.00	-224.322	69.685	-128.313
n-butyl acetate	-52.15	-4.070	83.75	0.00	-224.322	81.816	-114.979
pentyl acetate	-52.15	-3.841	83.75	0.00	-224.322	92.252	-104.314

<b>PEI</b>	<b>-52.15</b>	<b>-57.324</b>	<b>152.27</b>	<b>519.018</b>	<b>-498.494</b>	<b>24.213</b>	
		<b>R2</b>	<b>Pi</b>	<b>AH</b>	<b>BH</b>	<b>logL16</b>	
<b>ALKENES</b>							
propene		0.103	0.08	0.00	0.07	0.946	
1-butene		0.100	0.08	0.00	0.07	1.491	
1-pentene		0.093	0.08	0.00	0.07	2.013	
1-hexene		0.078	0.08	0.00	0.07	2.547	
1-heptene		0.092	0.08	0.00	0.07	3.063	
	<b>c</b>	<b>rR2</b>	<b>sPi</b>	<b>aAH</b>	<b>bBH</b>	<b>llogL16</b>	<b>logK'</b>
propene	-52.15	-5.904	12.18	0.00	-34.895	22.905	-57.860
1-butene	-52.15	-5.732	12.18	0.00	-34.895	36.102	-44.492
1-pentene	-52.15	-5.331	12.18	0.00	-34.895	48.741	-31.452
1-hexene	-52.15	-4.471	12.18	0.00	-34.895	61.671	-17.662
1-heptene	-52.15	-5.274	12.18	0.00	-34.895	74.164	-5.971

<b>PEI</b>	<b>-52.15</b>	<b>-57.324</b>	<b>152.27</b>	<b>519.018</b>	<b>-498.494</b>	<b>24.213</b>	
		<b>R2</b>	<b>Pi</b>	<b>AH</b>	<b>BH</b>	<b>logL16</b>	
<b>ALKANES</b>							
propane		0.000	0.00	0.00	0.00	1.050	
n-butane		0.000	0.00	0.00	0.00	1.615	
n-pentane		0.000	0.00	0.00	0.00	2.162	
n-hexane		0.000	0.00	0.00	0.00	2.688	
n-heptane		0.000	0.00	0.00	0.00	3.173	
	<b>c</b>	<b>rR2</b>	<b>sPi</b>	<b>aAH</b>	<b>bBH</b>	<b>llogL16</b>	<b>logK'</b>
propane	-52.15	0.000	0.00	0.00	0.000	25.424	-26.724
n-butane	-52.15	0.000	0.00	0.00	0.000	39.104	-13.044
n-pentane	-52.15	0.000	0.00	0.00	0.000	52.349	0.201
n-hexane	-52.15	0.000	0.00	0.00	0.000	65.085	12.937
n-heptane	-52.15	0.000	0.00	0.00	0.000	76.828	24.680

## Six Coating Comparison

### Selection of a Coating to Interact with Carboxylic Acids

	<b>c</b>	<b>r</b>	<b>s</b>	<b>a</b>	<b>b</b>	<b>l</b>	
<b>carb wax</b>	-2.07	0.25	1.40	2.13	-0.05	0.442	
<b>DEGS</b>	-1.81	0.12	1.76	1.84	0.11	0.399	
<b>PPE</b>	-2.54	0.04	1.01	0.53	0.08	0.554	
<b>TCEP</b>	-1.74	0.07	2.06	1.82	0.28	0.380	
<b>ZE7</b>	-2.10	-0.05	1.17	0.56	0.59	0.434	
<b>carb wax 20M</b>	-2.38	-2.44	2.85	9.39	-6.02	1.110	

	<b>R2</b>	<b>Pi</b>	<b>AH</b>	<b>BH</b>	<b>logL16</b>	
<b>acetic acid</b>	0.265	0.60	0.55	0.43	1.750	
<b>propanoic acid</b>	0.233	0.60	0.54	0.43	2.290	
<b>butanoic acid</b>	0.210	0.60	0.54	0.42	2.830	
<b>pentanoic acid</b>	0.205	0.60	0.54	0.41	3.380	
<b>hexanoic acid</b>	0.174	0.60	0.54	0.39	3.920	
<b>heptanoic acid</b>	0.149	0.60	0.54	0.38	4.460	

<b>CBWX</b>	<b>c</b>	<b>rR2</b>	<b>sPi</b>	<b>aAH</b>	<b>bBH</b>	<b>llogL16</b>	<b>logK'</b>
<b>acetic acid</b>	-2.07	0.066	0.840	1.172	-0.022	0.774	0.760
<b>propanoic acid</b>	-2.07	0.058	0.840	1.150	-0.022	1.012	0.969
<b>butanoic acid</b>	-2.07	0.053	0.840	1.150	-0.021	1.251	1.203
<b>pentanoic acid</b>	-2.07	0.051	0.840	1.150	-0.021	1.494	1.445
<b>hexanoic acid</b>	-2.07	0.044	0.840	1.150	-0.020	1.733	1.677
<b>heptanoic acid</b>	-2.07	0.037	0.840	1.150	-0.019	1.971	1.910

<b>DEGS</b>	<b>c</b>	<b>rR2</b>	<b>sPi</b>	<b>aAH</b>	<b>bBH</b>	<b>llogL16</b>	<b>logK'</b>
<b>acetic acid</b>	-1.81	0.032	1.056	1.012	0.047	0.698	1.035
<b>propanoic acid</b>	-1.81	0.028	1.056	0.994	0.047	0.914	1.229
<b>butanoic acid</b>	-1.81	0.025	1.056	0.994	0.046	1.129	1.440
<b>pentanoic acid</b>	-1.81	0.025	1.056	0.994	0.045	1.349	1.658
<b>hexanoic acid</b>	-1.81	0.021	1.056	0.994	0.043	1.564	1.867
<b>heptanoic acid</b>	-1.81	0.018	1.056	0.994	0.042	1.780	2.079

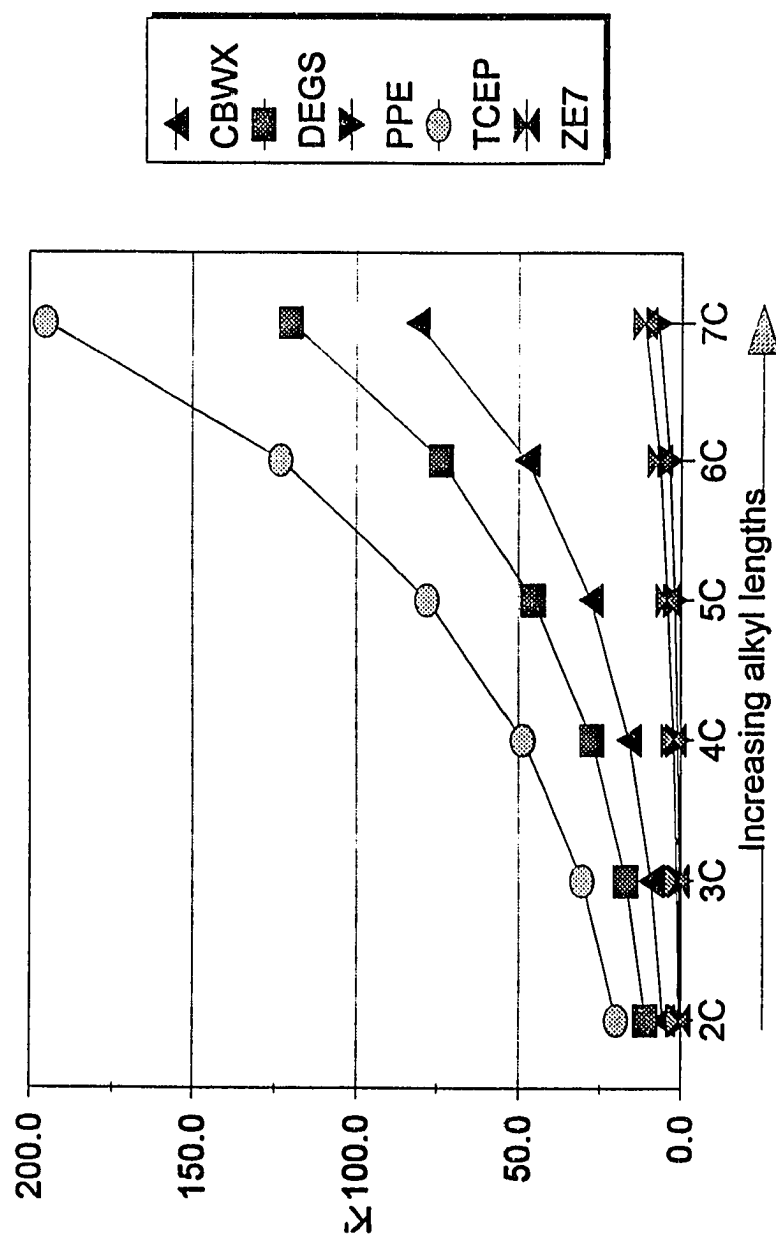
<b>PPE</b>	<b>c</b>	<b>rR2</b>	<b>sPi</b>	<b>aAH</b>	<b>bBH</b>	<b>llogL16</b>	<b>logK'</b>
<b>acetic acid</b>	-2.54	0.011	0.606	0.292	0.034	0.970	-0.628
<b>propanoic acid</b>	-2.54	0.009	0.606	0.286	0.034	1.269	-0.335
<b>butanoic acid</b>	-2.54	0.008	0.606	0.286	0.034	1.568	-0.038
<b>pentanoic acid</b>	-2.54	0.008	0.606	0.286	0.033	1.873	0.266
<b>hexanoic acid</b>	-2.54	0.007	0.606	0.286	0.031	2.172	0.562
<b>heptanoic acid</b>	-2.54	0.006	0.606	0.286	0.030	2.471	0.859

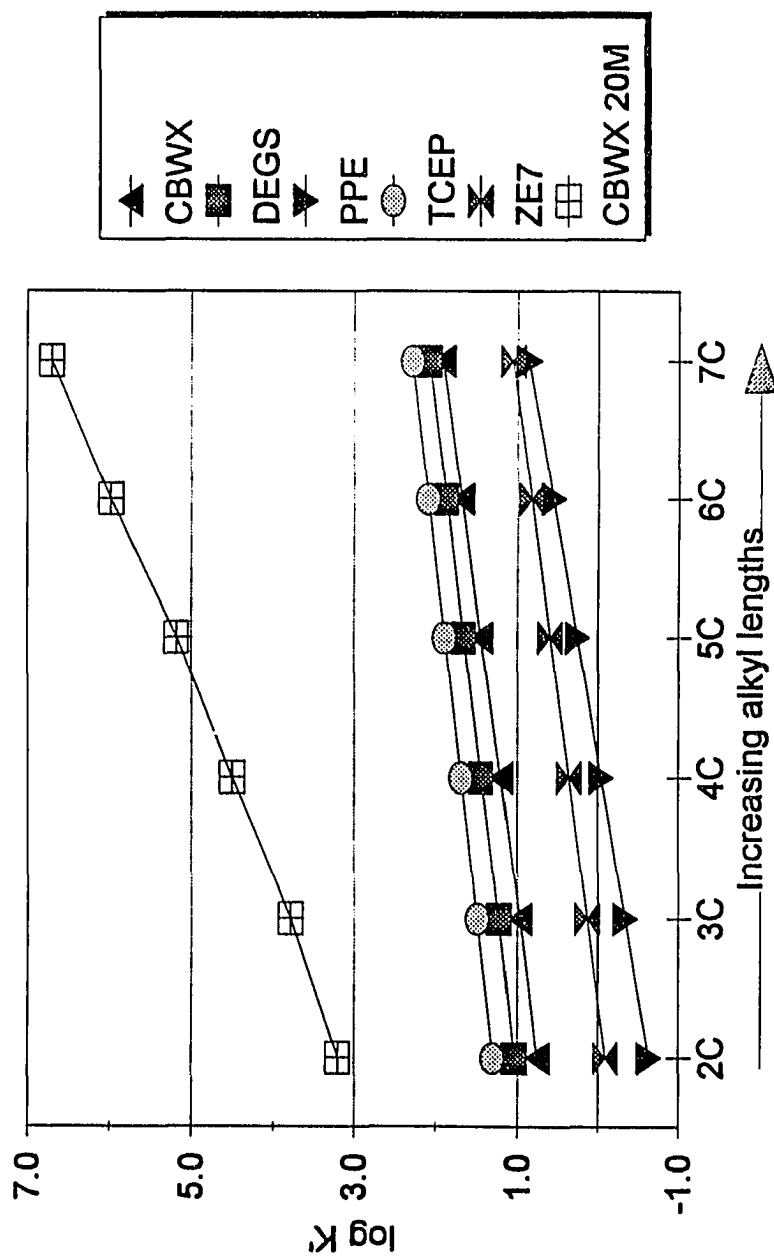
<b>TCEP</b>	<b>c</b>	<b>rR2</b>	<b>sPi</b>	<b>aAH</b>	<b>bBH</b>	<b>llogL16</b>	<b>logK'</b>
<b>acetic acid</b>	-1.74	0.019	1.236	1.001	0.120	0.865	1.301
<b>propanoic acid</b>	-1.74	0.016	1.236	0.983	0.120	0.870	1.486
<b>butanoic acid</b>	-1.74	0.015	1.236	0.983	0.118	1.075	1.687
<b>pentanoic acid</b>	-1.74	0.014	1.236	0.983	0.115	1.284	1.892
<b>hexanoic acid</b>	-1.74	0.012	1.236	0.983	0.109	1.490	2.090
<b>heptanoic acid</b>	-1.74	0.010	1.236	0.983	0.106	1.695	2.290

<b>ZE7</b>	<b>c</b>	<b>rR2</b>	<b>sPi</b>	<b>aAH</b>	<b>bBH</b>	<b>llogL16</b>	<b>logK'</b>
acetic acid	-2.1	-0.013	0.702	0.308	0.254	0.760	-0.090
propanoic acid	-2.1	-0.012	0.702	0.302	0.254	0.994	0.140
butanoic acid	-2.1	-0.011	0.702	0.302	0.248	1.228	0.370
pentanoic acid	-2.1	-0.010	0.702	0.302	0.242	1.467	0.603
hexanoic acid	-2.1	-0.009	0.702	0.302	0.230	1.701	0.827
heptanoic acid	-2.1	-0.007	0.702	0.302	0.224	1.936	1.057
<b>carbowax 20M</b>	<b>c</b>	<b>rR2</b>	<b>sPi</b>	<b>aAH</b>	<b>bBH</b>	<b>llogL16</b>	<b>logK'</b>
acetic acid	-2.38	-0.646	1.707	5.165	-2.588	1.943	3.201
propanoic acid	-2.38	-0.568	1.707	5.071	-2.588	2.543	3.784
butanoic acid	-2.38	-0.512	1.707	5.071	-2.528	3.142	4.500
pentanoic acid	-2.38	-0.500	1.707	5.071	-2.467	3.753	5.183
hexanoic acid	-2.38	-0.424	1.707	5.071	-2.347	4.353	5.979
heptanoic acid	-2.38	-0.363	1.707	5.071	-2.287	4.952	6.700

## Proposed Interaction Five Coatings with Six Acids



## Proposed Interaction Six Coatings with Six Acids



**APPENDIX III**

**MOLECULAR MODELING SOFTWARE  
INFORMATION**

### **Semi-Empirical Molecular Modeling Software**

The advent of high-technology computerization has revolutionized the field of computational chemistry. Beginning in the early 1970s, Norman L. Allinger developed and demonstrated that MM1 (Allinger) force field calculations could be offered as an acceptable methods for determining the structures and energies of molecules under many circumstances. The MM1 force field calculations incorporated such energy parameters as molecular stretching, bending, stretch bend, and van der Waals interactions. Initially these "first generation" force field calculations did not always coincide well with experimental data. A point of contention existed between whether it was the calculations, the experimental technique, or both, that were in error. In 1977, Allinger and colleagues developed the MM2 (QCPE-395, 1977) force field which included the torsional potentials in addition to the previously described parameters. Numerous semi-empirical software packages currently exist. Many utilize Allinger's force fields. Others, not discussed herein, may include the force fields of Schleyer (EAS) and Bartell (MUB-2). I have elected to describe one software package which utilizes a modified form of Allinger's original programs. This research plan is not limited to any one particular software package.



### **PCMODEL Software**

The force field used in PCMODEL software is called MMX and is derived from the MM2 force field of N.L. Allinger. It also utilizes the pi valence electron self consistent field (pi-VESCF) routines Allinger developed called MMP1. Modifications were made by J. McKelvey of Kodak to the pi-VESCF routines for open shell species while improvements to the heat of formation calculations were done by J.J. Gajewski. The number of atom types for the MM2 force field were increased by MMX. It also added the ability to handle transition metals and transition states, and increased the number of parameters included in the data base. J.J. Gajewski and K.E. Gilbert made these changes. In addition, PCMODEL contains a graphical interface and minimizer package. (Serena Software)

The current versions of PCMODEL vary according to their intended workstations. The PCMODEL-386 version running under DOS can handle up to 500 total atoms; whereas, PCMODEL for Silicon Graphics and IBM RS/6000 workstations can handle up to 10,000 atoms.

## Allinger's Force Field Parameters for MM2

### Stretching

$$E_s = 71.94 k_s (l - l_0)^2 [l - 2.00(l - l_0)]$$

where lengths are in Å,  $k_s$  is in mdyn/Å

### Bending

$$E_\theta = 0.021914 K_\theta (\theta - \theta_0)^2 [1 + 7.0(10)^{-8} (\theta - \theta_0)^4]$$

where  $\theta$  is in deg,  $k_\theta$  is in mdyn/Å rad<sup>2</sup>

### Stretch-Bend

$$E_{s_\theta} = 2.51124 k_{s_\theta} (\theta - \theta_0) [(l - l_0)_a + (l - l_0)_b]$$

where bond angles  $a$  and  $b$  are attached with an angle  $\theta$

### Van der Waals

$$E_v = \epsilon [2.90(10)^5 \exp(-12.50 / P) - 2.25 P^6]$$

where  $P$  = sum of Van der Waals radii ( $\Sigma r^*$ ) divided by the distance ( $r$ ) between interacting centers. For carbon the interacting center is at the nucleus; for hydrogen it is 0.915 of the bond length out from carbon. Note that the Van der Waals C | H distance is not (CC + H/H)/2

### Torsion

$$E_\omega = \frac{V_1}{2}(1 + \cos \omega) + \frac{V_2}{2}(1 - \cos 2\omega) + \frac{V_3}{2}(1 + \cos 3\omega)$$

where all torsional angles  $\omega$  are measured (0-180°) and included in the calculation.

## BIBLIOGRAPHY

- 
- (1) E. J. Poziomek and S. Chen, Submitted to the *Journal of Forensic Sciences*, November 1992
  - (2) T. Lukaszewski and W. K. Jeffery, *Journal of Forensic Sciences*, JFSCA, 1980, **25**, July, No. 3, 499
  - (3) H. L. Schlesinger, *Bulletin on Narcotics*, 1985, **37**, No. 1, 64
  - (4) *The Merck Index*, 11th Ed., S. Budavari (ed.), Merck & Co., Rahway, New Jersey, 1989, p. 383, #2450
  - (5) A. H. Lawrence, L. Elias, and M. Authier-Martin, *Canadian Journal of Chemistry*, 1984, **62**, 1886
  - (6) C. S. Wu, W. C. Beely, and S. D. Worley, *Journal of Computational Chemistry*, 1992, **12**, No. 7, 862
  - (7) M. Novak and C. A. Salemink, *Tetrahedon*, 1989, **45**, No. 13, 4287
  - (8) Y. Nakahara and A. Ishigami, *Journal of Analytical Toxicology*, 1991, May/June, **15**, 105
  - (9) S. Vishveshwara and J. A. Pople, *Journal. American Chemical Society*, 1977, **99**, 2422
  - (10) B. T. Luke, A. G. Gupta, G. H. Loew, J. G. Lawless, and D. H. White, *International Journal of Quantum Chemistry.: Quantitative Biological Symposium*, 1977, **11**, 117

- 
- (11) R. J. Hrynchuk, R. J. Barton, and B. E. Robertson, *Canadian Journal of Chemistry*, 1983, **61**, 481
- (12) A. Streitwieser and C. H. Heathcock, *Introduction to Organic Chemistry*, 2nd Ed., Macmillan, New York, New York, 1981, 725
- (13) A. W. Czanderna and C. Lu, *Methods and Phenomena 7 - Applications of Piezoelectric Quartz Crystal Microbalances*, C. Lu and A. W. Czanderna Ed., Elsevier, Amsterdam, 1984
- (14) A. W. Czanderna and C. Lu, *Methods and Phenomena 7 - Applications of Piezoelectric Quartz Crystal Microbalances*, C. Lu and A. W. Czanderna Ed., Elsevier, Amsterdam, 1984, Chapter 1, 2
- (15) C. Lu, *Methods and Phenomena 7 - Applications of Piezoelectric Quartz Crystal Microbalances*, C. Lu and A. W. Czanderna Ed., Elsevier, Amsterdam, 1984, Chapter 2, 19-61
- (16) L. L. Levenson, *Nuovo Cimento*, Suppl. 2, Ser. I, 1967, **5**, 321
- (17) G. Z. Sauerbrey, *Zeitschrift fuer Physik*, 1959, **155**, 206
- (18) G. Z. Sauerbrey, *Zeitschrift fuer Physik*, 1964, **178**, 457
- (19) G. G. Guilbault, *Methods and Phenomena 7 - Applications of Piezoelectric Quartz Crystal Microbalances*, C. Lu and A. W. Czanderna (Eds.), Elsevier, Amsterdam, 1984, Chapter 8, 251-252
- (20) C. D. Stockbridge, *Vacuum Microbalance Techniques*, Vol. 5, K. H. Behrndt (Ed.), Plenum, New York, NY, 1966, 217
- (21) L. Rohrschneider, *Journal of Chromatography*, 1966, **22**, 6

- 
- (22) W.O. McReynolds, *Journal of Chromatographic Science*, 1970, **8**, 685
- (23) E. Sz. Kovats, *Helvetica Chimica Acta*, 1958, **41**, 1915
- (24) A.J.P. Martin and R.L.M. Synge, *Biochemical Journal*, 1941, **35**, 91
- (25) A.J.P. Martin and R.L.M. Synge, *Biochemical Journal*, 1944, **37**, proc. xiii
- (26) A.T. James and A.J.P. Martin, *Biochemical Journal*, 1952, **50**, 679
- (27) J.W. Grate and M.H. Abraham, *Sensors and Actuators B*, 1991, **3**, 85-111
- (28) M. Janghorbani and H. Freund, *Analytical Chemistry*, 1973, **45**, 325-332
- (29) T.E. Edmunds and T.S. West, *Analytica Chimica Acta*, 1980, **117**, 147- 157
- (30) J.J. McCallum *et al.*, *Analytica Chimica Acta*, 1984, **162**, 75-83
- (31) J.W. Grate, A. Snow, D. S. Ballantine Jr., H. Wohltjen, M. H. Abraham, R. A. McGill, and P. Sasson, *Analytical Chemistry*, 1988, **60**, 869-875
- (32) A.B. Littlewood, *Gas Chromatography*, Academic Press, New York, 1970, Chapter 3, 71-85
- (33) A. Braithwaite and F.J. Smith, In *Chromatographic Methods*, Fourth Edition, Chapman & Hall, London, 1985, 161
- (34) L. Rohrschneider, *Journal of Chromatography*, 1966, **22**, 6

- 
- (35) W. McReynolds, *Journal of Chromatographic Science*, 1970, **8**, 685
- (36) S.K. Pool, B. R. Kersten, and C. F. Poole, *Journal of Chromatography*, 1989, **471**, 91
- (37) M.H. Abraham, G. S. Whiting, R. M. Doherty, W. J. Shuely, *Journal. Chemical Society (London). Perkin Transactions. II*, 1990, 1451
- (38) F. Patte, *Analytical Chemistry*, 1982, **54**, 2239
- (39) Dykstra, Clifford E., Electrostatic Interaction Potentials in Molecular Force Fields, *Chemical Reviews*, 1993, **93**, 2339-2353
- (40) W. Stumm and J. J. Morgan, In *Aquatic Chemistry - An Introduction Emphasizing Chemical Equilibria in Natural Waters*, 2nd Edition, John Wiley and Sons, New York, NY, 1981, 602
- (41) H. M. Fog and B. Reitz, Piezoelectric Crystal Detector for the Monitoring of Ozone in Working Environments, *Analytical Chemistry*, 1985, **57**, 2634
- (42) I. Langmuir, *Journal. American Chemical Society*, **40**, 1361 (1918)
- (43) R.H. Fowler and E.A. Guggenheim, *Statistical Thermodynamics*, Cambridge University Press, Cambridge, 1952, Chapt. 10
- (44) R. M. Rosenberg, *Principles of Physical Chemistry*, Oxford University Press, New York, NY, 1977, 662
- (45) S. Brunauer, P.H. Emmett, and E. Teller, *Journal. American Chemical Society*, 1938, **60**, 309

- 
- (46) T.L. Hill, Theory of Physical Adsorption, *Advances in Catalysis*, Academic, New York, 1952, IV, 225-242
- (47) T. L. Hill, *Journal of Chemical Physics*, 1946, **14**, 263 and 1949, **17**, 772
- (48) M. Dominguez, S. Lin, and J. Li, Harry Reid Center for Environmental Studies, University of Nevada, Las Vegas, Las Vegas, Nevada, 89154
- (49) H. Wohltjen, *Instructions for Vapor and Dilution Apparatus*, VG-400, Microsensor Systems Inc., Bowling Green, KY, 1993
- (50) W. H. King, *Analytical Chemistry*, 1964, **36**, No. 9, 1735